

# 1 **Assessing the simple dynamical systems approach in a** 2 **Mediterranean context: application to the Ardèche** 3 **catchment (France)**

4  
5 **M. Adamovic<sup>1,4</sup>, I. Braud<sup>1</sup>, F. Branger<sup>1</sup>, J.W. Kirchner<sup>2,3</sup>**

6 [1] Irstea, UR HHLY, Hydrology-Hydraulics Research Unit, Lyon-Villeurbanne, France

7 [2] Department of Environmental Systems Science, Swiss Federal Institute of Technology,  
8 ETH Zurich, Zurich, Switzerland

9 [3] Swiss Federal Research Institute WSL, Birmensdorf, Switzerland

10 [4] Hydrosiences, UMR 5569 CNRS-IRD-UM1&2, Université Montpellier 2, Montpellier,  
11 France

12 Correspondence to: M. Adamovic (marko.adamovic@hotmail.com)

## 14 **Abstract**

15 This study explores how catchment heterogeneity and variability can be summarized in  
16 simplified models, representing the dominant hydrological processes. It focuses on  
17 Mediterranean catchments, characterized by heterogeneous geology, pedology, and land use,  
18 as well as steep topography and a rainfall regime in which summer droughts contrast with  
19 high-rainfall periods in autumn. The Ardèche catchment (south-east France), typical of this  
20 environment, is chosen to explore the following questions: 1/ can such a Mediterranean  
21 catchment be adequately characterized by simple dynamical systems approach and what are  
22 the limits of the method under such conditions? 2/ what information about dominant  
23 predictors of hydrological variability can be retrieved from this analysis in such catchments?

24 In this work we apply the data-driven approach of Kirchner (WRR, 2009) to estimate  
25 discharge sensitivity functions that summarize the behavior of four sub-catchments of the  
26 Ardèche, using low-vegetation periods (November-March) from **9 years** of measurements  
27 (2000-2008) from operational networks. The relevance of the inferred sensitivity function is  
28 assessed through hydrograph simulations, and through estimating precipitation rates from  
29 discharge fluctuations. We find that the discharge sensitivity function is downward-curving in  
30 double-logarithmic space, thus allowing further simulation of discharge and non-divergence  
31 of the model, only during low-vegetation periods. The analysis is complemented by a Monte-

1 Carlo sensitivity analysis showing how the parameters summarizing the discharge sensitivity  
2 function impact the simulated hydrographs. The resulting discharge simulation results are  
3 good for granite catchments, which are likely to be characterized by shallow subsurface flow  
4 at the interface between soil and bedrock. The simple dynamical system hypothesis works  
5 especially well in wet conditions (peaks and recessions are well modeled). On the other hand,  
6 poor model performance is associated with summer and dry periods when evapotranspiration  
7 is high and low-flow discharge observations are inaccurate. In the Ardèche catchment,  
8 inferred precipitation rates agree well in timing and amount with observed gauging stations  
9 and SAFRAN climatic data reanalysis during the low-vegetation periods. The model should  
10 further be improved to include a more accurate representation of actual evapotranspiration,  
11 but provides a satisfying summary of the catchment functioning during wet and winter  
12 periods.

13

## 14 **1 Introduction**

15 Catchments show a high degree of heterogeneity and variability, both in space and time  
16 (McDonnell et al., 2007) raising questions about the degree of complexity that must be used  
17 to model their behavior (Sivapalan, 2003a). Many hydrological models are based on the  
18 bottom-up or reductionist approach (Sivapalan, 2003b; Zehe et al., 2006), following the  
19 blueprint proposed by Freeze and Harlan (1969). Governing equations such as the Darcy or  
20 Richards' equation, which are inherent in many hydrological models, are suitable for point-  
21 scale processes (Bloschl and Sivapalan, 1995; Kirchner, 2006). Their use to describe  
22 processes at larger scales leads to the calibration of "effective parameters" which are  
23 sometimes difficult to link with measurable quantities (Sivapalan, 2003b), although recent  
24 methods combining the use of small-scale variability and regionalization techniques were  
25 shown to be efficient in preserving spatial patterns of variability (Samaniego et al., 2010).  
26 Such "effective" large-scale equations might not, however, describe hydrologic processes  
27 realistically, even if they can be calibrated to reproduce observed catchment behavior  
28 (Kirchner, 2006). Klemeš (1983) was one of the first hydrologists proposing the use of  
29 alternative modeling concepts. He defines the top-down or downward approach as the "*route*  
30 *that starts with trying to find a distinct conceptual node directly at the level of interest (or*  
31 *higher) and then looks for the steps that could have led to it from a lower level*". To go in this  
32 direction, Sivapalan (2003b) and Kirchner (2006) promote a combination of data analysis and  
33 process conceptualization (the top-down approach). This allows understanding the main

1 drivers of the system functioning (the perceptual model; Beven, 2002) and inferring the  
2 system's "emergent properties" (Sivapalan, 2003b) or "functional traits" (McDonnell et al.,  
3 2007). Thus, models obtained through this approach are simple, with a limited number of  
4 parameters that can be estimated from the available data.

5 Kirchner (2009) represents a catchment with a simple bucket model in which system  
6 parameters are derived directly from measured streamflow fluctuations during recession  
7 periods. He based his analysis on storage-discharge relationships with one essential  
8 assumption: discharge depends only on the total water stored in the catchment. This approach  
9 allows the derivation of a first-order non-linear differential equation for simulating rainfall-  
10 runoff behavior. Until now, this approach has mostly been applied in small, humid  
11 catchments. Kirchner (2009) obtained good results for the Severn (8.70 km<sup>2</sup>) and Wye (10.55  
12 km<sup>2</sup>) catchments at Plynlimon, in Mid-Wales. Teuling et al. (2010) also applied this approach  
13 to the prealpine Rietholzbach catchment (3.31 km<sup>2</sup>) getting good results in wet periods and  
14 poor model performance during dry periods. The study of Brauer et al. (2013) showed similar  
15 results for the Dutch lowland Hupsel Brook catchment (6.5 km<sup>2</sup>) where discharge results were  
16 correctly reproduced only in certain periods. Melsen et al. (2014) determined the minimum  
17 amount of data required to find robust parameter values for a simple Kirchner (2009) model  
18 with two parameters in the prealpine Rietholzbach catchment (3.31 km<sup>2</sup>). They concluded that  
19 a two-parameter model is reasonably able to capture high flows but they fail to describe the  
20 low flows.

21 Krier et al. (2012) applied the concept of doing hydrology backwards to infer spatially  
22 distributed rainfall rates in the Alzette catchment (1092 km<sup>2</sup>) in Luxembourg, and found that  
23 introducing a soil moisture threshold led to model improvement, especially under the wet  
24 conditions. However, they didn't simulate hydrographs. In addition, all those studies used  
25 data from well-monitored experimental catchments and, the method has not previously been  
26 applied using data from operational networks, which are much more common.

27 To our knowledge, the simple dynamical system approach (SDSA) proposed by Kirchner  
28 (2009) has not been evaluated in a Mediterranean context, where the rainfall regime exhibits  
29 strong contrasts between dry conditions in summer and intense rainfall events, often related to  
30 stationary Mesoscale Convective Systems (Hernández et al., 1998), during autumns.  
31 Wittenberg and Sivapalan (1999), for instance, used recession analyses to estimate  
32 groundwater recharge in a Mediterranean type of climate in Australia, but they did not

1 consider the storage-discharge relationship in its implicit differential form, the sensitivity  
2 function  $g(Q)$ .

3 Mediterranean catchments are also characterized by heterogeneous topography, vegetation and  
4 geology. The study of the water cycle in such Mediterranean conditions, as well as a better  
5 understanding and modelling of processes triggering flash floods, are central research topics  
6 addressed in the HyMeX<sup>1</sup> (Hydrological Cycle in the Mediterranean Experiment, Drobinski et  
7 al. (2013)) program and in the FloodScale<sup>2</sup> project (Braud et al., 2014), to which this study  
8 contributes.

9 Our study area is the Ardèche catchment (2388 km<sup>2</sup>, see location in Fig. 1), which is typical of  
10 Mediterranean catchments with highly variable rainfall, steep slopes, and heterogeneous  
11 geology and pedology. It is one of the studied catchments of the Cévennes-Vivarais Hydro-  
12 Meteorological Observatory (OHM-CV, Boudevillain et al. (2011)). Previous studies in this  
13 catchment mainly focused on flood forecasting and discharge quantile estimation. Discharge  
14 time series from the Ardèche catchment were used to assess the value of new observations in  
15 estimating extreme quantiles, such as information derived from paleofloods (Sheffer et al.,  
16 2002), historical floods (Lang et al., 2002; Naulet et al., 2005) or post-flood survey peak  
17 discharge estimates (Gaume et al., 2009). Flood forecasting studies extended to the whole  
18 Cévennes-Vivarais region are numerous and include work by Sempere-Torres et al. (1992),  
19 Duband et al. (1993), Le Lay and Saulnier (2007), Saulnier and Le Lay (2009), Trambly et  
20 al. (2010), and Garambois et al. (2013). Use of distributed hydrological models for process  
21 understanding during flash floods in the Cévennes-Vivarais region is more recent. Examples  
22 of such studies are those of Bonnifait et al. (2009), Manus et al. (2009), and Braud et al.  
23 (2010). Those studies use a reductionist approach to gain insight into active hydrological  
24 processes during floods and highlight a lack of data or parameter information.

25 As a complementary approach to the modeling studies mentioned above, we adopt in this  
26 study the data-based approach proposed by Kirchner (2009) to estimate the hydrological  
27 water balance of the Ardèche catchment and to gain insight into the dominant associated  
28 processes. Like in the work of Melsen et al. (2014), we divided our examined period into  
29 vegetation (April-October) and low-vegetation period (November-March) where  
30 evapotranspiration can be considered as a low.

---

<sup>1</sup> [www.hymex.org](http://www.hymex.org)

<sup>2</sup> <http://floodscale.irstea.fr/>

1 The idea is to use this insight to propose simple models with very few parameters to learn  
2 more about hydrological functioning at the catchment scale.

3 In the present paper, we focus on the following questions: 1/ what is the applicability of  
4 simple dynamical system approach (SDSA) and what are its limitations in a Mediterranean  
5 type catchment like the Ardèche with its particular conditions (size, climate, geological and  
6 pedological heterogeneity), and when data from operational networks are used? 2/ what can  
7 we learn about dominant hydrological processes using this methodology?

8 To answer those questions, we first estimate the discharge sensitivity function using the  
9 available discharge data. Then we assess the relevance of the obtained function by testing how  
10 well the simple model based on it can simulate observed discharge, and can retrieve rainfall.  
11 The study is complemented by examining the sensitivity of the results to the parameters of the  
12 discharge sensitivity function.

13

## 14 **2 Field Site and Data**

### 15 **2.1 The Ardèche catchment**

16 The Ardèche catchment is located in southern France (Fig. 1). The catchment has an area of  
17 2388 km<sup>2</sup>, and the Ardèche river itself has a length of 125 km. There are two main tributaries  
18 in the Ardèche basin: the Baume and Chassezac Rivers, which join the Ardèche River close to  
19 one another. Elevation ranges from the mountains of the Massif Central (highest point: 1681  
20 m) in the northwest, to the confluence with the Rhone River (lowest point: 42 m) in the  
21 southeast.

22 The main lithologies found in the Ardèche are schist, granite, and limestone (Fig. 2).  
23 Upstream, the Ardèche flows from west to east in a deep granite valley, then flows through  
24 basalt formations and schist in a north-south direction. Downstream, it flows through bedded  
25 and massive limestone before flowing into the Rhone River (see for example the description  
26 provided by Naulet et al. (2005)).

27 Among the land use types found in the Ardèche, forest dominates throughout the basin  
28 (Corine Land Cover database<sup>3</sup>). Forest is represented by a mix of coniferous (27%), broadleaf  
29 (13%) and Mediterranean trees (17%). Shrubs and bushes are also well represented in the  
30 catchment, occupying a significant portion of the area (17%). We also distinguish significant

---

<sup>3</sup> <http://sd1878-2.sivrit.org/>

1 areas of bare soil in the central and southern part of the Ardèche, as well as a few small urban  
2 areas and areas of early and late crops.

3 In the Ardèche basin, there is a strong influence of the Mediterranean climate with seasonally  
4 heavy rainfall events during autumn. Historical data show that these events usually lead to  
5 flash floods (Lang et al., 2002). Lang et al. (2002) mention seven rainfall events locally  
6 exceeding 400 mm during the 1961-1996 period. They also comment on the relatively quick  
7 flow response (a couple of hours) to precipitation due to the steepness of the upstream part of  
8 the catchment and presence of granitic and basaltic rocks.

9 Fig. 3 shows the average hourly regime of the main terms of the water balance equation for all  
10 months between 2000-2008, differently colored with respect to vegetation (red) and low-  
11 vegetation periods (blue). Under the main terms of the water balance we consider discharge,  
12 evapotranspiration and precipitation. As we consider interannual values, change in water  
13 storage is assumed to be zero. This hypothesis is consistent with the lack of a regional aquifer  
14 in the Ardèche catchment. The hydrological year consists mainly of two periods. There is a  
15 rainy season (September-February) with maximum precipitation intensity in autumn,  
16 characterized by rainfall amounts greatly exceeding reference evapotranspiration  $ET_0$   
17 (calculated based on the SAFRAN reanalysis of Quintana-Seguí et al. (2008): see next  
18 section), and by high discharge. On the other hand, during the dry season (March-August), on  
19 average  $ET_0$  is much larger than precipitation and runoff is low. Evapotranspiration is  
20 influenced by the seasonal cycles of temperature, radiation and vegetation, the latter being  
21 particularly marked in the Ardèche catchment, which is mostly covered by forests (around  
22 60 % of the total catchment area, with 27% of the forest being coniferous and thus remaining  
23 green even in winter).

## 24 **2.2 Available data and first data consistency analysis**

### 25 **2.2.1 Observations used in the study**

26 In the Ardèche catchment, measurements of the hydrological state variables have mainly been  
27 started in the 1960s for the purpose of flood forecasting. In our study, we use hourly data of  
28 precipitation ( $P$ ), reference evapotranspiration ( $ET_0$ ) and discharge ( $Q$ ) from the period 1 Jan  
29 2000 until 31 Dec 2008. These data come from operational networks, and not from research  
30 catchments as in previous applications of the SDSA, which renders the study challenging and

1 interesting, as operational networks account for a large fraction of the available discharge data  
2 in many regions.

3 The analysis is mostly constrained by the availability of discharge data, which were obtained  
4 from the national Banque Hydro website ([www.hydro.eaufrance.fr](http://www.hydro.eaufrance.fr)) and Electricité de France  
5 ([france.edf.com/](http://france.edf.com/)). Unfortunately, numerous dams and hydro-power stations are located in the  
6 upper parts of the Ardèche and Chassezac catchments (Fig. 1). These dams are used to  
7 regulate the water level throughout the year, in particular to ensure a sufficient discharge in  
8 the river for recreational use in the summer period. Data to reconstruct natural discharge at the  
9 hourly time step were not available. Thus we had to discard several gauging stations located  
10 downstream of the dams in order to apply the simple dynamical system approach to data  
11 where the water balance can be closed.

12 As the stations were not designed and managed for low flow measurements, the low-flow  
13 time series were investigated by contacting the operational services in charge of the stations.  
14 Consequently, two stations had to be removed from further analysis due to unreliable  
15 measurements and agriculture water withdrawals in summer periods. Ultimately, four sub-  
16 catchments could be examined: the Ardèche at Meyras (#1), the Borne at Nicolaud Bridge  
17 (#2), the Thines at Gournier Bridge (#3), and the Altier at Goulette (#4); see locations in Fig.  
18 1. These four sub-catchments are characterized by steep slopes (>15%), average altitude of  
19 around 1000 m and igneous and metamorphic bedrock. We have also computed Strahler  
20 stream order and channel length using TauDEM tools (Tarboton et al., 2009) in order to  
21 classify and measure the size of the river network. The analysis was conducted using the 25 m  
22 resolution IGN DTM and the D8 flow direction algorithm, so the resulting network statistics  
23 may only loosely resemble those that would be obtained from more accurate procedures such  
24 as field mapping. Main physiographic catchment characteristics are summarized in Table 1.

25 The discharge data were available at varying time intervals, and were aggregated to hourly  
26 sums. Two types of precipitation data have been examined and are used throughout the  
27 analysis. Local rain gauges at the hourly time step provided by the OHM-CV data base  
28 (Boudevillain et al., 2011) are used as the primary source of rainfall data for the catchment  
29 Ardèche at Meyras (#1). For the catchments Borne at Nicolaud Bridge (#2), Thines at  
30 Gournier Bridge (#3) and Altier at Goulette (#4), we use the SAFRAN reanalysis of Météo-  
31 France, based on 8 by 8 km<sup>2</sup> grids (Quintana-Seguí et al., 2008; Vidal et al., 2010) since either  
32 the local rain gauge shows lack of data and time gaps, or there is no rain gauging station in the  
33 catchment (e.g. Thines at Gournier Bridge (#3)). These precipitation data are calculated as

1 catchment averages at hourly time steps. To compute the reference evapotranspiration  $ET_0$ , we  
2 also used the climate variables of the SAFRAN reanalysis of Météo-France at an hourly time  
3 step.  $ET_0$  is calculated using the Penman-Monteith formula according to FAO  
4 recommendations (Allen et al., 1998). In order to account for vegetation type, we compute  
5 potential evapotranspiration ( $PET$ ) as reference evapotranspiration  $ET_0$  modulated by a crop  
6 coefficient depending on the nature of vegetation for each catchment (Eq. (1)).

$$7 \quad PET = K_C \times ET_0 \quad (1)$$

8 We also took into account the seasonal variability of vegetation through the definition of three  
9 crop coefficient stages: initial (01 January- 01 April), mid-season (15 April- 15 October) and  
10 late season (01 November- 31 December). Periods between initial and mid-season as well as  
11 between mid-season and late season are interpolated linearly. The values of crop coefficients  
12 for the Ardèche catchments were obtained through the FAO database (Allen et al., 1998). For  
13 each catchment we determined the cover estimates for each vegetation type (Broad-leaf forest,  
14 Mediterranean forest, Coniferous forest, Early crops, Late crops, Shrubs and bushes and Bare  
15 soil) and we calculated a weighted average crop coefficient per sub-catchment for each stage  
16 (see Table 2). Reference evapotranspiration  $ET_0$  and  $ET_0$  modulated by the crop coefficient  
17 ( $K_C ET_0$ ) over examined period (2000-2008) are given in Table 3.

### 18 **2.2.2 Data consistency**

19 To further assess data quality, we evaluated the consistency of the local rainfall station with  
20 SAFRAN data for the Ardèche at Meyras (#1) catchment at the hourly time step. The  
21 resulting coefficient of determination was 0.99. For the rest of the sub-catchments, we first  
22 assumed that SAFRAN rainfall is representative of the catchment average. However, by  
23 looking at the mean annual water fluxes (Table 3) and estimated runoff coefficients, we infer  
24 that the mass balances for catchments #2, #3 and #4 are implausible.

25 For these reasons, two actual evapotranspiration ( $AET$ ) estimates and runoff coefficients are  
26 provided to gain useful insight about data uncertainty. In Table 3 the first evapotranspiration  
27 estimate comes from the water balance  $AET_{WB} = P - Q$ , where  $P$  is the average annual  
28 precipitation and  $Q$  the annual runoff, assuming that change in water storage is null. In Table  
29 3, the first runoff coefficient ( $C$ ) is calculated as the ratio between  $Q$  and  $P$ . We also note that  
30  $AET_{WB}$  shows either high underestimation (#2 and #4) or overestimation (#3) in comparison  
31 with the  $K_C ET_0$  data, which once again points out the water balance closure issue.



1 In Table 4 the second  $AET$  estimate corresponds to Turc (1951) annual actual  
2 evapotranspiration, which is calculated using the following formula:

$$3 \quad AET_{Turc} = \frac{P}{\sqrt{0.9 + \frac{P^2}{L^2}}} \quad (2)$$

4 where  $P$  is annual precipitation in mm/year and  $L = 300 + 25T + 0.05T^3$  ( $T$  is the average  
5 annual temperature in  $^{\circ}\text{C}$ ). Here, the second runoff coefficient ( $C_{Turc}$ ) is calculated using the  
6 following equation:

$$7 \quad C_{Turc} = \frac{P - AET_{Turc}}{P} \quad (3)$$

8 where  $C_{Turc}$  is the runoff coefficient,  $P$  is precipitation (mm/y) and  $AET_{Turc}$  is the actual Turc  
9 evapotranspiration (mm/y). We use  $AET_{Turc}$  in this formula along with precipitation in order to  
10 estimate annual runoff coefficients in the examined catchments.

11 The values of the water balance components differ from catchment to catchment as illustrated  
12 in Table 3. By comparing the Table 3 and 4, we note that the mass balance  $AET_{WB}$  and  $AET_{Turc}$   
13 estimates are only consistent for the Ardèche at Meyras (#1) catchment; at the other three sites  
14 they differ greatly, leading to inconsistent runoff coefficients for the same catchment. This  
15 suggests that either the rainfall or  $ET_0$  (or possibly both) are not representative at the other  
16 catchments. Regarding rainfall, the gridded SAFRAN product is known to underestimate  
17 precipitation in mountainous areas and to underestimate the occurrence of strong  
18 precipitation, which could help to explain the water balance closure problems (see Sect. 5.1  
19 for more details).

20 Discharge data uncertainty has been addressed in many works and sometimes it can be quite  
21 large, especially in catchments where high flows are seldom gauged due to safety reasons (Le  
22 Coz et al., 2010) or where low flows may be difficult to measure accurately. Nevertheless,  
23 here we decided to go ahead with the available operational discharge data, to assess if the  
24 SDSA can provide useful information about catchment hydrological functioning in a  
25 Mediterranean context, even in the presence of some uncertainty in the discharge data.

26 However, in order to apply the SDSA with data where water balance closure is more  
27 representative, we rescaled precipitation and  $K_c ET_0$  values for catchments (#2, #3 and #4).  
28 Our rescaling scheme (see next section for more details) assumes that the discharge data were  
29 accurate enough for the application of the SDSA, which relies mainly on discharge data.

## 1 2.3 Rescaling of water balance fluxes

2 The first step in the rescaling analysis was to obtain a robust estimate of actual  
3 evapotranspiration.

4 We used following equation of Fu (1981) to draw Budyko (1974) type curves for the Ardèche  
5 catchments:

$$6 \frac{AET}{P} = 1 + \frac{ET_0}{P} - \left[ 1 + \left( \frac{ET_0}{P} \right)^w \right]^{\frac{1}{w}} \quad (4)$$

7 where  $AET/P$  is the evapotranspiration ratio,  $ET_0/P$  is the dryness index and  $w$  is a catchment  
8 parameter.

9 The parameter  $w$  was empirically derived by Fu (1981) and it can have values from  $[1 \sim \infty]$ .  
10 Zhang et al. (2004) defined parameter  $w$  as a coefficient representing “*the integrated effects of*  
11 *catchment characteristics such as vegetation cover, soil properties and catchment topography*  
12 *on the water balance*”.

13 In our study, we drew Fu curves with parameter  $w$  ranging between 1.5 and 5 to get an insight  
14 about evapotranspiration ratios in the Ardèche. The next step was to compare those curves  
15 with mean actual annual evapotranspiration ratios obtained using the Turc (1951), Schreiber  
16 (1904), Pike (1964) and Budyko formulae (see Table 5). We note from Fig. 4 that almost all  
17 calculated  $AET/P$  ratios lie in a  $w$  range between 1.7 and 3. On the other hand, the  $AET$   
18 estimates derived using  $AET_{WB}=P-Q$  (cyan color in Fig. 4) for catchments #2, #3 and #4 were  
19 found to lie outside the range of values given by the various formulae, highlighting the water  
20 balance problem. Finally, to assess and adjust our data sets ( $P$  and  $AET$ ), we chose Turc  
21 inferred evapotranspiration as representative for future analysis. In the 1951 paper, Turc  
22 reports an evaluation of his formula by comparing measured interannual discharge to values  
23 estimated through  $P-AET$  where  $AET$  is estimated by formula (2) of the paper with generally  
24 good performance. The considered data set covered countries all over the world. Thus, relying  
25 only on the  $P$  and  $T$  and not on  $ET_0$ , we could avoid the use of evapotranspiration and reduce  
26 uncertainty in estimating  $AET$ . In addition, the Turc equation is widely used in France to  
27 estimate  $AET$ , and thus our results can be compared to other studies.

28 We then make the following assumptions. We assume that the long-term average  $Q$  is valid.  
29 We also assume that the “relative” day-to-day variations of  $K_c ET_0$  and  $P$  are valid, but that the  
30 mean  $P$  does not reflect the whole-catchment  $P$ , and the mean  $K_c ET_0$  does not reflect the mean  
31  $AET$ . Therefore the means need to be rescaled to achieve a consistent set of measurements. As

1 mentioned before, we assume that the **Turc (1951)** formula correctly describes the relationship  
2 between average  $AET$  and average  $P$ . Then we iteratively solve the Turc formula to find long-  
3 term average  $AET_{Turc}$  and  $P_{Turc}$  that are consistent with one another, and consistent with the  
4 average  $Q$ .

5 The hourly precipitation values are then rescaled by multiplying them by the ratio found in the  
6 previous step between the average  $P_{Turc}$  and the average measured  $P$ . Secondly, the  $ET_0$   
7 values are also rescaled by multiplying the hourly  $K_c ET_0$  by the ratio found between the  
8 average  $AET_{Turc}$  and the initial  $K_c ET_0$  estimate. **The improved AET estimate is  $AET = \alpha_{AET} *$**   
9  **$K_c ET_0$  where  $\alpha_{AET}$  is the scaling AET factor provided in Table 4. While this scaling factor is**  
10 **assumed to be constant throughout the year, hourly variation (hourly  $ET_0$  signal) and seasonal**  
11 **variations (seasonal  $K_c$ ) of AET are considered. Assuming one mean annual value of  $\alpha_{AET}$  is**  
12 **coarse, as strong seasonal variations in AET signal are expected due to the seasonal variations**  
13 **of  $ET_0$  and vegetation activity, but water balances (and thus  $\alpha_{AET}$  estimates) would be more**  
14 **uncertain over shorter periods.** Table 4 shows the results of data rescaling for catchments #2,  
15 #3 and #4 that have unrealistic mass balances. It gives the values of the computed rescaled  
16  $AET_{Turc}$  and the corresponding computed mean annual precipitation ( $P_{Turc}$ ). In addition,  
17 scaling parameter values,  $\alpha_{AET}$  and  $\alpha_P$  are given for each considered catchment. **We consider**  
18 **the rescaled runoff coefficients to be more realistic, as they are closer to those of catchment**  
19 **#1, where the water balance is consistent with Turc (1951) AET.**

20 The new precipitation and new AET values for catchments #2, #3 and #4 are then used in  
21 further analysis, whereas original data were conserved only for catchment #1.

22

### 23 **3 Methodology**

24 In this part, we first present the estimation of the discharge sensitivity function,  $g(Q)$ , which is  
25 used to characterize the catchment hydrological response. Then we assess whether the  
26 estimated  $g(Q)$  is really representative of the catchment behavior using two additional  
27 calculations. First, a simple bucket deterministic model is built for the various examined sub-  
28 catchments and simulated discharge is compared to observations. Second, rainfall catchment  
29 amounts are retrieved from discharge fluctuations ("doing hydrology backwards") and  
30 compared to independent observations. Afterwards, we present a sensitivity analysis showing  
31 the impact of the parameters of the  $g(Q)$  function on the results. Finally, Kirchner's approach

1 is used with non-rescaled precipitation and evapotranspiration data to show how data  
2 **inconsistency** problems may affect discharge simulations.

### 3 **3.1 Estimation of the sensitivity function $g(Q)$**

4 Kirchner (2009) proposed a method for determining non-linear reservoir parameters for a  
5 simple bucket model with the assumption that discharge  $Q$  depends uniquely on total water  
6 storage  $S$  in the catchment. The analysis starts, as many parametric rainfall-runoff models do,  
7 with the water balance equation, in which the total catchment storage variation is estimated  
8 using:

$$9 \frac{dS}{dt} = P - AET - Q \quad (5)$$

10 where  $S$  is water storage volume (L) and  $P$ ,  $AET$ , and  $Q$  are rates of precipitation, actual  
11 evapotranspiration, and discharge, respectively ( $L T^{-1}$ ).  $Q$ ,  $P$ ,  $AET$  and  $S$  are considered as  
12 functions of time and considered to be averaged over the whole catchment (Kirchner, 2009).

13 It is known that precipitation measurements are spatially variable. Rain gauges reflect  
14 precipitation on areas much smaller than the catchment itself. The same comment is valid for  
15 evapotranspiration estimates, which are typically representative of much smaller areas than  
16 the catchment.

17 In Eq. (5), only discharge can be considered as a state variable that characterizes the entire  
18 catchment. This observation led Kirchner (2009) to make the fundamental assumption that  
19 discharge is uniquely dependent on total water storage  $S$  in the catchment, and that therefore:

$$20 Q = f(S) \text{ OR } S = f^{-1}(Q) \quad (6)$$

21 Differentiating Eq. (6) with respect to time, one obtains:

$$22 \frac{dQ}{dt} = \frac{dQ}{dS} \frac{dS}{dt} = \frac{dQ}{dS} (P-AET-Q) \quad (7)$$

23 **and  $dQ/dS$  can also be expressed as a function of  $Q$ , following Kirchner (2009), as:**

$$24 \frac{dQ}{dS} = f'(S) = f'(f^{-1}(Q)) = g(Q) \quad (8)$$

25 where  $g(Q)$  is the “sensitivity function” as defined in Kirchner (2009). It describes the  
26 sensitivity of discharge to changes in storage, as a function of discharge itself. This is useful  
27 because discharge is directly measurable whereas whole-catchment storage is not.

28 Combining Eq. (7) and Eq. (8) we can express  $g(Q)$  as (Kirchner, 2009):

$$29 g(Q) = \frac{dQ}{dS} = \frac{dQ/dt}{dS/dt} = \frac{dQ/dt}{P-AET-Q} \quad (9)$$

1 where the sensitivity function can be described using precipitation ( $P$ ), actual  
2 evapotranspiration ( $AET$ ), discharge ( $Q$ ) and rate of change of discharge ( $dQ/dt$ ).

3 Following the approach of Kirchner (2009), we consider periods when precipitation and  
4 actual evapotranspiration are relatively small compared to discharge, obtaining the following  
5 equation, which shows that under these conditions the discharge sensitivity function can be  
6 estimated from discharge data alone:

$$7 \quad g(Q) = \frac{dQ}{dS} \approx -\frac{dQ/dt}{Q} \Big|_{P \ll Q, AET \ll Q} \quad (10)$$

8 We select hourly records for nighttime (defined as the period between sunset and sunrise)  
9 during which the total rainfall is less than 0.1 mm within the preceding 6 h and following 2 h  
10 (Krier et al., 2012). We also tested larger time windows (10 and 12 hours instead of 8 hours)  
11 which did not improve  $g(Q)$  estimation.

12 The sensitivity function  $g(Q)$  is estimated using discharge records from low-vegetation  
13 periods (from November to March) from 2000 until 2008, when vegetation and  $ET_0$  could be  
14 considered to have a smaller impact on stream discharge. Melsen et al. (2014) also pointed out  
15 the importance of selecting the low-vegetation periods for estimating the  $g(Q)$  function due to  
16 the high evapotranspiration conditions in the rest of the year. They also suggest that one  
17 winter season could be enough to get a robust estimate of  $g(Q)$ . Given the larger catchment  
18 size and larger climate variability in our catchment, we use the whole low-vegetation period  
19 from 2000-2008 for this estimation. Later, the resulting  $g(Q)$  function was nevertheless used  
20 for precipitation retrieval and discharge simulation during both low-vegetation and vegetation  
21 periods (April-October).

22 We avoid the vegetation period for the estimation of the  $g(Q)$  function since, as Fig. 3 shows,  
23 during this period  $ET_0$  is much larger than discharge, and the Ardèche catchments clearly  
24 respond to  $ET_0$  forcing during the entire 24 hour period. In addition, in the Ardèche basin, the  
25 diurnal amplitude (computed as half the difference between the daily maximum and minimum  
26 flow) often exceeds 20 % of the daily average flow.

27 These rainless nighttime hours are further used to determine the sensitivity function  $g(Q)$  by  
28 constructing "recession plots" (Brutsaert and Nieber, 1977) of the flow recession rate ( $-dQ/dt$ )  
29 as a function of discharge. Following Brutsaert and Nieber (1977) and Kirchner (2009), the  
30 flow recession rate is estimated as the difference between two successive hours as:

$$31 \quad \frac{-dQ}{dt} = \frac{(Q_{t-\Delta t} - Q_t)}{\Delta t} \quad (11)$$

1 Then, the discharge is averaged over those two hours as  $(Q_{t-\Delta t} + Q_t)/2$ . Binning is then done  
 2 by grouping the individual hourly data into ranges of  $Q$  and then calculating the mean and  
 3 standard error for  $-dQ/dt$  and  $Q$  for each bin. Following Kirchner (2009), values of  $-dQ/dt \leq 0$   
 4 are also included in the binning analysis to avoid the introduction of bias. The bin size was  
 5 initially set at 1% of the logarithmic range in  $Q$  but was locally increased if necessary to bring  
 6 the standard error of  $-dQ/dt$  down to 50% of the mean  $-dQ/dt$  (Kirchner, 2009).

7 A quadratic function (Kirchner, 2009) is then fitted to the binned means leading to the  
 8 following empirical equation in log space:

$$9 \quad \ln(g(Q)) = \ln\left(-\frac{dQ/dt}{Q} \Big|_{P < Q, AET < Q}\right) \approx C_1 + C_2 \ln(Q) + C_3 (\ln(Q))^2 \quad (12)$$

10 As noted by Kirchner (2009), the  $C_2$  parameter in the Eq. (12) is one less than the linear term  
 11 in a regression fit to the binned  $\ln(-dQ/dt)$  versus  $\ln(Q)$  plot.

## 12 **3.2 Discharge simulation**

13 Discharge sensitivity functions can be used to simulate discharge (Kirchner, 2009) by  
 14 combining Eq. (9) and Eq. (10), resulting in the following expression, where the quadratic  
 15 function of Eq. (12) is used to describe  $g(Q)$ :

$$16 \quad \frac{dQ}{dt} = \frac{dQ}{ds} \frac{ds}{dt} = g(Q)(P - AET - Q) \quad (13)$$

17 In solving Eq. (13), attention is paid to two details, time lags and numerical instabilities  
 18 (Kirchner, 2009). A time lag is introduced to account for flow routing delays between changes  
 19 in catchment storage and changes in discharge at the outlet. Changes in subsurface storage  
 20 could also lag behind rainfall inputs due to the delays necessary for rainfall to infiltrate and  
 21 change discharge at the outlet. However, these time lags do not affect the estimation  $g(Q)$   
 22 since  $Q$  and  $dQ/dt$  are measured simultaneously at the catchment outlet.

23 Eq. (13) indicates that  $dQ/dt$  depends on the balance between precipitation, actual  
 24 evapotranspiration and discharge. However, variations in  $P-AET-Q$  are mainly forced by  
 25 variations in precipitation. For instance, in the Ardèche at Meyras (#1) catchment, the  
 26 variance of hourly precipitation is over 15 times larger than the variance of hourly discharge  
 27 and around 80 times larger than the variance of hourly evapotranspiration. In discharge  
 28 simulations, lag time is not of such importance since discharge is highly auto-correlated.  
 29 However, in precipitation retrieval, lag time is taken into account to enhance model  
 30 performance (see Sect. 3.3 for more details) because precipitation varies more on short time  
 31 scales.

1 In order to minimize numerical instabilities, Eq. (13) is solved using its log transform  
2 (Kirchner, 2009):

$$3 \frac{d(\ln(Q))}{dt} = \frac{1}{Q} \frac{dQ}{dt} = \frac{g(Q)}{Q} (P - AET - Q) = g(Q) \left( \frac{P - AET}{Q} - 1 \right) \quad (14)$$

4 Eq. (14) is then computed using fourth-order Runge-Kutta integration, iterating on an hourly  
5 time-step. A single value of measured discharge is used to initialize the simulation. In  
6 addition, Kirchner (2009) also remarked that solution can be unstable unless the parameter  $C_3$   
7 of Eq. (12) is less than 0.

8 To estimate the  $AET$  term in Eq. (14), Kirchner (2009) originally used Penman-Monteith  
9 reference evapotranspiration and a rescaling effective parameter ( $k_e$ ) that was calibrated for  
10 the entire study period. Other authors have used slight variants of this approach: Teuling et al.  
11 (2010) used the Priestley-Taylor equation to estimate catchment-scale evapotranspiration,  
12 defining the evaporation efficiency as a fitting parameter; Brauer et al. (2013) used a  
13 parameter  $f$  that takes into account the difference between potential and actual  
14 evapotranspiration on a monthly basis.

15 In our study, we assumed that actual evapotranspiration is equal to potential  
16 evapotranspiration ( $PET$ ) throughout the year, being defined as reference evapotranspiration  
17  $ET_0$  modulated by a crop coefficient depending on the nature of vegetation for each catchment  
18 (Eq. (1)). The strong hypothesis that  $AET = PET$  is likely to be more relevant in winter, when  
19 there is sufficient water content in the air and soils, than in summer. For example, Boronina et  
20 al. (2005) found that in Cyprus, actual evapotranspiration was close to potential rate during  
21 the November-March period since there was always water present in the air and soils.  
22 Nonetheless we use this assumption, even in summer, as a first rough approximation in order  
23 to assess the feasibility of such a simple modeling concept. For the application to the Ardèche  
24 catchment, as mentioned in Sect. 2.2.1, we assumed that  $AET$  was given by Eq. (1), computed  
25 on an hourly time step. According to the catchment, either the original  $K_C ET_0$  (catchment #1)  
26 or rescaled  $\alpha_{AET} K_C ET_0$  (catchments #2, #3, #4) were used.

27 To show how data inconsistency problems may affect the performance of discharge  
28 simulation, we also ran the model with non-rescaled values of precipitation and  
29 evapotranspiration. The resulting model performance is reported in Sect. 4.5.

### 1 3.3 Rainfall retrieval based on $g(Q)$

2 Until recently, it was considered infeasible to infer precipitation from stream flow  
3 fluctuations. **Spatial** variability of precipitation is high and conventional rain-gauges can only  
4 measure precipitation over an area that is many orders of magnitude smaller than a catchment  
5 itself. We assess the relevance of the inferred storage-discharge relationship for the examined  
6 catchments in the Ardèche using the rainfall retrieval scheme (“doing hydrology backward”)  
7 as proposed by Kirchner (2009) and further tested by Krier et al. (2012).

8 Assuming that the assumptions of the SDSA are valid, we can infer temporal patterns of  
9 precipitation rates from streamflow fluctuations using the following inversion of Eq. (13), as  
10 outlined by Kirchner (2009):

$$11 \quad P - AET = \frac{dS}{dt} + Q = \frac{dQ/dt}{dQ/dS} + Q = \frac{dQ/dt}{g(Q)} + Q \quad (15)$$

12 To apply this concept, one must take account of the travel time lag between changes in  
13 discharge from the hillslope and changes in stream flow at the outlet. A time-lag  $l$  is used for  
14 this purpose leading to the following equation (Kirchner, 2009):

$$15 \quad P - AET \approx \frac{(Q_{t+l+1} - Q_{t+l-1})/2}{[g(Q_{t+l+1}) + g(Q_{t+l-1})]/2} + (Q_{t+l+1} - Q_{t+l-1})/2 \quad (16)$$

16 where  $l$  is the travel time lag.

17 The time lag is optimized for each sub-catchment by calculating the correlation coefficient  
18 between estimated and measured rainfall using the lag times of 1, 2, 3, 4, 5, 6, 12, 24 and 48  
19 hours. The lag time that shows the best correlation is used. This approach is similar to the one  
20 used by Krier et al. (2012).

21 To make this concept of “doing hydrology backward” feasible, we identify periods when the  
22 contribution of evapotranspiration in the water balance equation can be neglected. This  
23 includes rainy periods when relative humidity should be relatively high, resulting in low  
24 evapotranspiration fluxes and thus  $P - AET \approx P$ . Based on this assumption, precipitation rates  
25 can be directly deduced from the stream flow fluctuations using the following formula  
26 (Kirchner, 2009):

$$27 \quad P \approx \text{MAX} \left( 0, \frac{(Q_{t+l+1} - Q_{t+l-1})/2}{[g(Q_{t+l+1}) + g(Q_{t+l-1})]/2} + (Q_{t+l+1} - Q_{t+l-1})/2 \right) \quad (17)$$

28 where  $P$  is the precipitation rate retrieved from discharge fluctuations with time lag  $l$ .

29 To measure the agreement between the reference values and the retrieved values we use the  
30 coefficient of determination  $R^2$  (see Sect. 3.4 for more details). The reference precipitation is



1 defined as a combination of local rain gauging and SAFRAN estimates depending on the sub-  
2 catchment being examined (see Sect. 2.2).

### 3 **3.4 Comparison between observed and simulated/retrieved values**

4 To assess model efficiency, we use Nash-Sutcliffe efficiency and percent bias as model  
5 evaluation criteria for discharge simulations, and coefficient of determination for rainfall  
6 retrieval. Nash-Sutcliffe efficiency,  $NSE$  (Nash and Sutcliffe, 1970) is used as a dimensionless  
7 model evaluation statistic indicating how well the simulated discharges fit the observations.  
8 We compute the  $NSE$  to emphasize the high flows as shown in the following equation:

$$9 \quad NSE = 1 - \left( \frac{\sum_{i=1}^n (Y_i^{obs} - Y_i^{sim})^2}{\sum_{i=1}^n (Y_i^{obs} - Y^{mean})^2} \right) \quad (18)$$

10 where  $Y_i^{obs}$  is the  $i$ -th observation of discharge data,  $Y_i^{sim}$  is the simulated discharge value for  $i$ -  
11 th time step,  $Y_i^{mean}$  is the mean of all observed data and  $n$  represents the number of  
12 observations.

13  $NSE$  values range between  $-\infty$  and 1.0, with 1 representing the optimal value (see Moriasi et  
14 al., 2007, for a recent review of performance criteria). We also computed  $NSE$  on the  
15 logarithm of the discharge to give less weight to the peaks.

16 In addition, percent bias ( $PBIAS$ ) was also calculated as a part of the model evaluation  
17 statistics. It measures total volume difference between two time series, as Eq. (19) indicates:

$$18 \quad PBIAS = \frac{\sum_{i=1}^n (Y_i^{obs} - Y_i^{sim}) * 100}{\sum_{i=1}^n (Y_i^{obs})} \quad (19)$$

19 where  $Y_i^{obs}$  is the  $i^{\text{th}}$  observation of discharge data,  $Y_i^{sim}$  is the simulated discharge value for the  
20  $i^{\text{th}}$  time step,  $n$  represents the number of observations and 100 converts the result to percent.

21 The optimal value of  $PBIAS$  is 0.0 where positive values indicate model overestimation bias,  
22 and negative values indicate model underestimation bias (e.g. Gupta et al., 1999).

23 In rainfall retrieval, model performance is assessed by using the coefficient of determination  
24 ( $R^2$ ) to quantify the linear correlation between observed and inferred precipitation.  $R^2$  ranges  
25 from 0 to 1, where higher values indicate smaller error variance (e.g., Moriasi et al., 2007).  
26 Although the inversion formula yields individual hourly values (Eq. 14), we use daily  
27 averages to compute  $R^2$ . This is done to reduce the effects of small discrepancies in timing  
28 that become less consequential when  $R^2$  is calculated on a daily time step (Kirchner, 2009).

### 1 **3.5 Sensitivity analysis**

2 In this part, we performed a Monte-Carlo analysis to sample the parameter space defined by  
3 the three parameters  $C_1$ ,  $C_2$  and  $C_3$  and investigate further whether the values derived from  
4 stream flow fluctuations are representative, and how these parameters impact streamflow  
5 simulations. This Monte-Carlo sensitivity study was conducted for the Ardèche at Meyras  
6 (#1) catchment.

7 A representative set of 10 000 ( $C_1$ ,  $C_2$ ,  $C_3$ ) triplets was sampled randomly from the *a priori*  
8 defined parameter ranges (see Sect. 4.4 for more details) using Monte Carlo methods. Then  
9 the discharge was simulated using the model presented in Sect. 3.2 and Eq. (14). We used the  
10 Nash Sutcliffe efficiency (*ln* for low flow and *linear* for high flows) to measure the similarity  
11 between the simulated and observed discharge. Then we verified that the parameter set  
12 derived from data is in the range of the sets leading to the best agreement between model and  
13 observations.

14 The number of simulations (10 000) was assumed to be adequate in view of the relative  
15 simplicity of the parametric model, and because the best-fit *NSE* did not change significantly  
16 beyond 10 000 simulations. For comparison, Zhang et al. (2008) and Tekleab et al. (2011)  
17 used 20 000 simulations for a four-parameter dynamic water balance model, and Uhlenbrook  
18 et al. (1999) used more than 400 000 model runs for the much more complex HBV model  
19 with 12 parameters.

20

## 21 **4 Results**

22 The results section is divided into five parts. In the first part, results concerning estimation of  
23  $g(Q)$  function and its sensitivity analysis are given. Then we present the assessment of the  
24 relevance of this estimated  $g(Q)$  function by examining the accuracy of the simulated  
25 discharge (Sect. 4.2) and retrieved precipitation (Sect. 4.3). In Sect. 4.4, the impact of  
26 parameter variations on the simulated hydrographs and results of the Monte-Carlo simulations  
27 are shown. Finally, the results with non-scaled original data are presented in Sect. 4.5.

### 28 **4.1 $g(Q)$ estimation**

29 Fig. 5 shows an example of a recession plot for the Ardèche at Meyras (#1) catchment for the  
30 all low-vegetation periods between 2000 and 2008. We observe that the recession plot exhibits  
31 large scatter at low discharge. This result is consistent with the findings of Kirchner (2009)

1 and Teuling et al. (2010). They argue that this is possibly due to measurement errors or  
2 differences between the modeling concept and reality.

3 Table 6 provides values of the recession plot parameters for all four catchments during low-  
4 vegetation periods between 2000 and 2008. It shows one parameter set for each catchment.  
5 We observe that our choice of the low-vegetation period for estimation of  $g(Q)$  gives  
6 consistent results amongst different catchments, with similar values of parameters  $C_1$  and  $C_2$ .  
7 We also observe that the  $C_3$  parameter, which controls the downward/upward curving of the  
8  $g(Q)$  function, is always negative, ranging from -0.02 up to -0.2. This is important because  
9 Kirchner (2009) obtained realistic simulated discharge only when recession plots are  
10 downward-curving on a log-log scale (meaning the  $C_3$  parameter is negative). Eventually,  
11 these parameter sets allowed stable discharge simulation as can be seen in Sect. 4.2.

12 We have also tested  $g(Q)$  estimation for all vegetation periods between 2000 and 2008; during  
13 these periods, the  $C_3$  parameter tended to be positive. In this case, when the  $g(Q)$  function is  
14 extrapolated to very low discharges, very high values of  $g(Q)$  are obtained, and thus,  
15 numerical instabilities appear that led to model non-functionality. This is also probably  
16 due to the distortion of the discharge time series by evapotranspiration as explained in Sect.  
17 3.1. Melsen et al. (2014) concluded that a two-parameter "bucket" model is reasonably able to  
18 capture high flows but not low flows. In our analysis we used the three-parameter model  
19 where the third parameter  $C_3$  is essentially related to the low flows (see Sect. 4.4.1) in order to  
20 capture the catchment behavior in that flow regime.

## 21 4.2 Discharge simulations

22 Continuous discharge simulations were performed for 2000-2008. Fig. 6 presents a simulation  
23 extract (year 2004) for the Ardèche at Meyras (#1) catchment. Table 7 presents a model  
24 performance summary ( $NSE$ ,  $NSE$  of the logarithm of discharge, and  $PBIAS$ ) for each  
25 catchment and each year.

26 Looking at Fig. 6, we can see that discharge simulations reproduce the observed hydrograph  
27 behavior better in winter and low-vegetation periods. The low-flow (summer) periods are less  
28 well reproduced, even if the overall performance of the simulation is good. The influence of  
29 evapotranspiration in summer periods can be one of the explaining factors for that. It should  
30 be noted that high evapotranspiration influence is visible only when discharge is evaluated in

1 log space. In linear space, evapotranspiration has a negligible influence on (already quite  
2 small) discharge, and the model runs well under dry conditions.

3 We note in Table 7 that the Ardèche at Meyras (#1) catchment shows satisfactory performance  
4 with  $NSE=0.68$ ,  $NSE\ log=0.74$  and  $PBIAS$  of 7.9 % for the nine-year simulation period.  
5 Unsatisfactory performance is observed for 2005 ( $NSE=-0.15$ ,  $NSE\ log=0.07$  and  $PBIAS$  of  
6 62.2 %). Year 2005 in general can be characterized as a dry year with annual precipitation of  
7 775 mm and annual reference evapotranspiration of 947 mm for this catchment. A mean  
8 annual precipitation of 1621 mm and mean evapotranspiration of 809 mm across the  
9 examined period (2000-2008) clearly confirms that year 2005 can be considered unusually  
10 dry. Table 7 also shows that the year-to-year variations in NSE are very large with some very  
11 good results in some years and poor results in other years. This could be a major challenge if  
12 the model were to be used for operational purposes.

13 Furthermore, Gupta et al. (1999) show that  $PBIAS$  values for streamflow tend to vary more  
14 than other performance criteria between dry and wet years. This could be another possible  
15 explanation of the overall poor model performance in 2005 for the Ardèche at Meyras  
16 catchment. The Borne at Nicolaud Bridge (#2) and Thines at Gournier Bridge (#3) catchments  
17 show good overall performance for the nine-year period with  $NSE=0.67$  and  $NSE\ log=0.61$   
18 and  $NSE=0.55$  and  $NSE\ log=0.78$  respectively. These catchments have stronger variations in  
19  $PBIAS$ , however. The last catchment, Altier at Goulette (#4) shows satisfactory model  
20 performance with  $NSE=0.74$  and  $NSE\ log=0.18$ . It is not known whether the low  $NSE\ log$   
21 value reflects poor model performance or unreliable low-flow discharge data.

### 22 **4.3 Precipitation retrieval**

23 Following Kirchner's approach we retrieved precipitation from discharge fluctuations. We  
24 used the same  $g(Q)$  derived from the low-vegetation periods (2000-2008) to infer  
25 precipitation rates in both vegetation and low-vegetation periods.

26 The coefficient of determination, mean bias, and slope of the relationship between inferred  
27 and measured rainfall for examined catchments and low-vegetation periods, as well as  
28 information about lag time, can be found in Table 8. Other lag times ( $> 2$  hours) showed poor  
29 model performance and are not discussed further in the paper.

1 Fig. 7 shows daily precipitation retrieval for the four studied sub-catchments of the Ardèche  
2 during low-vegetation periods, vegetation periods and for the entire study period 2000-2008  
3 using the same  $g(Q)$  function estimated from low-vegetation periods (Table 6).

4 Good correlation between retrieved precipitation and observed precipitation can be observed  
5 for low-vegetation periods where the slope of the regression line shows a modest degree of  
6 over-estimation. Fig. 7 illustrates that the inferred precipitation daily totals from low-  
7 vegetation periods (blue line) agree quite well with the precipitation measurements in the  
8 Altier at Goulette (#4) catchment, yielding  $R^2$  of 0.72. In the other catchments, the inferred  
9 precipitation daily totals are well correlated with the either local precipitation measurements  
10 or SAFRAN data, showing however sometimes a strong tendency toward overestimation  
11 (e.g., the Ardèche at Meyras, #1). Fig. 7 also shows strong precipitation overestimation for  
12 three examined catchments #1, #2 and #3 in summer periods (red line) and consequently for  
13 total examined period too (green line).

14 The optimized time lags are generally very small (less than 2 hours), which confirms the very  
15 short response time in the Ardèche catchment. In order to see whether the retrieved daily  
16 rainfalls were sensitive to the lag time, we compared the results obtained with different lag  
17 times for two catchments: the Ardèche at Meyras (#1) and Altier at Goulette (#4). The  
18 Ardèche at Meyras (#1, 98 km<sup>2</sup>) has an optimized lag time of 2 hours. We tested the retrieval  
19 behavior with lag times of 1 and 2 hours and we observe almost no change in the performance  
20 (Table 8): we obtain the same coefficient of determination of 0.41 and a bias of 7.9 mm d<sup>-1</sup> at  
21 a lag time of 1 and 2 hours. Similar results are obtained for the Altier at Goulette (#4)  
22 catchment, where we observed a slightly better precipitation modeling performance with lag  
23 time of 1 hour ( $R^2=0.72$ ) rather than with a lag time of 2 hours ( $R^2=0.71$ ).

## 24 **4.4 Sensitivity analysis**

### 25 **4.4.1 Impact of parameter variations on the simulated hydrographs**

26 As a first approach, a manual sensitivity analysis was done by successively varying the values  
27 of each parameter and plotting the corresponding simulated hydrographs (grey areas in Figs. 8  
28 and 9). The results for the Ardèche at Meyras (#1) catchment (year 2004) are presented; see  
29 Fig. 8 and Fig. 9 for the  $C_3$  and  $C_1$  parameters, respectively. The results for the parameter  $C_2$   
30 are not presented here since this parameter only varies slightly when estimated from low-  
31 vegetation periods in each year (see Sect. 4.1) and the results are graphically quite similar to

1 those for the parameter  $C_1$  (but peaks are less affected). The  $NSE$  values of log discharge are  
2 also calculated (Table 9).

3 We can see that  $C_3$  seems to be influential during the low-flow summer period and also during  
4 recessions of events following low-flow periods (Fig. 8). However, it does not play a  
5 significant role in the peaks and in well-established high-flow conditions. In contrast, the  $C_1$   
6 parameter has an important influence on the whole hydrograph (Fig. 9), including the peaks.  
7 Low values of  $C_3$  tend to flatten the model response, causing overestimated low-flow values  
8 and underestimated peaks.

9 From Table 9 we can also observe that the model efficiency for the parameter values that were  
10 obtained from the recession plots is close to optimal (at least for this year at this site), and  
11 cannot be substantially improved by manual parameter adjustments.

#### 12 **4.4.2 Exploration of parameter range using Monte-Carlo simulations**

13 In order to complement the manual sensitivity analysis presented above, to explore the range  
14 of these parameters and to assess whether the parameters of the  $g(Q)$  function-derived from  
15 data analysis are representative, we performed Monte-Carlo simulations using the model  
16 described by Eq. (14) with randomly sampled values of the three parameters  $C_1$ ,  $C_2$  and  $C_3$ .  
17 The parameters were sampled randomly from the *a priori* defined parameter range given in  
18 Table 10. For each simulation, the  $NSE$  and  $NSE \log$  (on the log of discharge) were calculated  
19 to assess the performance of the parameter set. The results are presented using dot plots for  
20 the Ardèche at Meyras (#1) catchment in Fig. 10. Table 10 also indicates the range of  
21 “behavioral” values for each parameter as derived from the dot plots, defined as the range  
22 where  $NSE$  is higher than 0.7, along with the values derived from the recession plots.

23 The results show that when the parameters are calibrated to discharge simulations, their  
24 ranges are quite large. The maximum model performance appears to be around 0.8 for all  
25 three parameters and both indicators. Low-flow performance ( $NSE \log$ ) is not very sensitive  
26 to the variations of the parameters. Giving peak flow more weight ( $NSE$ ) allows the  
27 identification of clear optima and a narrower range for the  $C_1$  parameter. Concerning the  $C_2$   
28 parameter, although the initial guess of the parameter range was quite narrow (see Table 10),  
29 the final “optimized” range is almost the same, with no clear optimum. For the  $C_3$  parameter,  
30 the final “optimized” range is found to be the half of the initial one. These two parameters  
31 appear thus to be not very sensitive, although the sign of the  $C_3$  parameter was already  
32 identified as a key element of successful discharge simulations. Finally, the parameter values

1 obtained from recession plots are in the optimized parameter range, thus suggesting that the  
2 analysis of discharge recessions is sufficiently informative and that there is no need of  
3 additional model calibration for discharge simulation. Beven and Binley (1992) have argued  
4 that having too many parameters increases the degrees of freedom beyond what data can  
5 properly deal with; this results in having different sets of parameters that give similar results  
6 (the equifinality problem). Fig. 10 shows that although conventional parameter calibration  
7 leads to substantial equifinality (particularly for the  $C_2$  parameter), the parameter values  
8 obtained from the recession plots fit well within the "behavioral" parameter range from the  
9 Monte Carlo analysis. Our analysis shows that the recession plots yield parameter estimates  
10 that are consistent with (and arguably better constrained than) parameter values obtained from  
11 conventional model calibration methods.

#### 12 **4.5 Modeling performance with non-scaled original data**

13 In Sect. 2.3 we introduced a rescaling technique to obtain more representative water balances  
14 for catchments #2, #3 and #4. Here, we show the consequences of foregoing this rescaling for  
15 those three catchments that showed unrealistic mass balances (Table 3). Fig. 11 shows  
16 observed discharge and simulated hourly hydrographs for the Altier at Goulette (#4)  
17 catchment for the year 2000, obtained with non-scaled data, rescaling of precipitation alone,  
18 and rescaling of both precipitation and evapotranspiration.

19 The lack of water balance closure may contribute substantially to poor model performance, as  
20 can be seen from Fig. 11. The simple dynamical systems approach, like many modeling  
21 approaches, is based on conservation of mass; it is therefore unsurprising that it may perform  
22 poorly when tested against data sets that violate mass conservation. We observe that when the  
23 original non-scaled data are used, discharge is generally underestimated. By introducing the  
24 rescaled precipitation, flow peaks can be better reproduced, but model performance is still  
25 poor during the vegetation period. If both the rescaled evapotranspiration and rescaled  
26 precipitation are used, significantly better results are obtained in both vegetation and low-  
27 vegetation periods.

28 As a complement to assessing modeling performance with non-scaled data, we re-ran the  
29 SDSA model for these catchments to see how this affects the hydrograph simulation and  
30 performance indicators. Table 11 compares model performance with the original operational  
31 data and the rescaled data, using *NSE*, *NSE on log of discharge* and *PBIAS* as performance  
32 metrics. We observe that model performance is markedly improved by using the rescaled

1 precipitation as forcing (runoff coefficients are more representative as shown in Table 4). In  
2 addition, model performance is improved by also introducing rescaled evapotranspiration  
3 (better *NSE* and lower *PBIAS* values are obtained).

## 5 Discussion

6 In this study, the Kirchner (2009) approach was applied to four sub-catchments in the Ardèche  
7 catchment (France), representative of **Western** Mediterranean catchments. We first discuss the  
8 advantages and limits of the method for this type of catchment. Then we discuss how the  
9 application of this approach was useful in deriving information about the catchment  
10 functioning and possible dominant processes.

### 5.1 About the applicability of the SDSA to Mediterranean type catchments

12 The application of this method to the Ardèche catchment was at first quite challenging. In  
13 particular, the basins are larger and **less humid** than those of the original case studies; in  
14 addition, data availability is more limited and data quality is distinctly lower.

#### - drainage area

16 The drainage area does not seem to be a limiting factor at the scale of our catchments. The  
17 catchments where this theory has been applied so far in order to reproduce the hydrograph  
18 were typically smaller than  $\sim 10 \text{ km}^2$ . In our study, the sizes of the studied catchments varied  
19 from  $16 \text{ km}^2$  to  $103 \text{ km}^2$  and SDSA approach performance was not correlated to the size of the  
20 catchment. Krier et al. (2012) report that when this approach is used for “doing hydrology  
21 backward” to retrieve rainfall amounts, the model performance in larger basins is as good as  
22 or sometimes even better than in smaller catchments. Kirchner (2009) also addressed this  
23 issue arguing that the approach was unlikely to work for catchments that are too big (e.g.  
24 more than  $1000 \text{ km}^2$ ). This is due to the lag times required for changes in discharge to reach  
25 the outlet; in such large catchments these lag times would be so long and variable that the  
26 model would be likely to fail. In addition, the theory presented here could not be expected to  
27 work in the catchments that are bigger than the scale of individual storms (Kirchner, 2009).  
28 Suggestions for how to deal with large river basins are given in Sect. 6.

#### - data quality

30 Our study demonstrates that data quality is particularly important for the application of this  
31 method. Concerning discharge data, the method is based on the discharge-sensitivity function



1  $g(Q)$ , and discharge measurement errors consequently will lead to biases in the appraisal of  
2 the catchment functioning. In catchments with artificial reservoirs/dams the assumption of a  
3 unique storage-discharge relation will not hold from the SDSA point of view. Thus this will  
4 limit the applicability of the SDSA method (and many other catchment models) in practice.

5 In the present study, we used discharge data from operational networks. We have shown in  
6 Sect. 2.2 that there are known issues with the quality of these data for our purposes.  
7 Nevertheless, when data consistency is sufficient (e.g. Ardèche at Meyras (#1) station), a  
8 robust estimation of the  $g(Q)$  function from low-vegetation periods can be obtained, leading  
9 to accurate simulation of the discharge. In addition, we would like to emphasize that the  
10 discharge sensitivity function  $g(Q)$  only depends on discharge. Its estimation is therefore not  
11 dependent on the rescaling performed on rainfall and  $ET_0$  data. There is only a minor impact  
12 of this rescaling on the selection of points retained for the recession plots; rainfall thresholds  
13 are used in this selection, but the results are only marginally impacted by rescaling. On the  
14 other hand, rescaling is of paramount importance in the evaluation of the relevance of the  
15 estimated  $g(Q)$  function using discharge simulation, as shown in Sect. 4.5., because accurate  
16 discharge simulations require that mass is conserved.

17 The quality of the rainfall data was questioned early in our work, and rescaling of  
18 precipitation was needed to obtain realistic results. As mentioned in Sect. 2.2, the gridded  
19 SAFRAN product underestimates precipitation especially in mountainous areas and  
20 underestimates the occurrence of strong precipitation ( $P > 20 \text{ mm day}^{-1}$  (Quintana-Seguí et  
21 al., 2008; Vidal et al., 2010). As the SAFRAN reanalysis is performed on so-called  
22 “symposium zones”, assumed to be homogeneous in terms of climate characteristics,  
23 overestimation of rainfall is also possible if those zones are inaccurately delineated, as is  
24 probably the case for the Thines at Gournier bridge (#3) catchment. Some authors tried to  
25 overcome the rainfall underestimation problem in mountainous areas by interpolating the  
26 SAFRAN data across altitude bands (Etchevers et al., 2001; Lafaysse et al., 2011; Thierion et  
27 al., 2012), but these data were not available for the present study. In addition, SAFRAN re-  
28 analyses are based on existing rain gauges. In mountainous areas, the few rain gauges that do  
29 exist are generally located in lower, flatter terrain, and may not capture the increase of rainfall  
30 with altitude that has been identified in this region (Molinié et al., 2011). It would be  
31 interesting to assess the performance of the “hydrology backwards” rainfall inversion using  
32 more accurate rainfall estimates as reference. As reference daily rainfall, we propose to use

1 the SPAZM reanalysis (Gottardi, 2009), which improves rainfall estimation in mountainous  
2 area, when it becomes available to us.

3 Assuming that the discharge data are reliable, it was shown that when input rainfall and  $ET_0$   
4 consistent with the water balance closure are used, the discharge simulated using the  $g(Q)$   
5 function is much more accurate than with the original input data. Coussot (2015) generalized  
6 the study presented in this paper to about 20 catchments of the Cévennes region and found the  
7 same kind of water balance closure problems as in our study. Once rescaling of rainfall and  
8  $ET_0$  was performed, he obtained similar results as those presented in this paper.

9 One assumption behind the rescaling approach proposed in Sect. 2.2.2 is that discharge data  
10 are reliable enough to provide an accurate estimate of annual runoff. This is of course  
11 questionable, because stage-discharge relationships are known to be highly extrapolated in  
12 this region due to the difficulty of gauging high discharges (e.g. Le Coz et al., 2010). As also  
13 mentioned in Sect. 2.2.1, low discharges are also highly uncertain, because these stations were  
14 often designed for flood warning purposes. Work is currently in progress in order to quantify  
15 the runoff data accuracy. This work is based on the BaRatin method (Le Coz et al., 2014)  
16 which provides an uncertainty range on the estimated discharge. The uncertainty can be  
17 propagated to the whole discharge time series (Branger et al., 2015) and the next step will be  
18 the propagation to the hydrological water balance and the quantification of uncertainty for the  
19 annual and monthly values. This work will help quantify which of the data (rainfall, discharge  
20 or both) need to be improved.

21 In addition, the operational discharge measurement network has recently been complemented  
22 by research instrumentation covering nested scales (see Braud et al., 2014 for details). In  
23 particular, small catchments ranging from 0.5 to 100 km<sup>2</sup> have been monitored continuously  
24 since 2010. The data set was not long enough to be used in the present study, but these new  
25 data are expected to be of higher accuracy than the operational data used in this study, so that  
26 they can provide additional insight into the hydrological response of the catchments.

27 Regarding discharge uncertainty, if data have to be rescaled, an approach like the one  
28 proposed by Yan et al. (2012) should be preferred, as it allows a consolidation of the water  
29 balance at the scale of the whole Ardèche catchment, taking into account data uncertainties on  
30 all the components, and constraining the results with the water balance equation along the  
31 river network.

1 The simulation results show that additional effort must be put into quantifying data  
2 uncertainty in both discharge and rainfall. The derivation of more accurate rainfall fields  
3 combining various data sources (such as radar data and in situ gauges (see, for instance,  
4 Delrieu et al. 2014) should also be encouraged. It could also be interesting to use actual  
5 evapotranspiration estimates derived from remote sensing techniques adapted to complex  
6 topography (e.g., Gao et al., 2011; Seiler and Moene, 2010) to obtain independent estimates of  
7 *AET* and better constrain this component in hydrological modeling.

8

### 9 - adequacy of SDSA in our catchment

10 The sampling strategy of deriving the  $g(Q)$  functions from low-vegetation periods appeared to  
11 be adequate in our case. We estimated  $g(Q)$  by using the streamflow data from low-vegetation  
12 periods of the 9-year time series (2000-2008) and then used the resulting parameterization to  
13 reproduce the hydrographs (continuous simulations) for the rest of the 9-year interval. This  
14 procedure can be understood as a “differential split-sample test” (Klemes, 1986) where the 9-  
15 year-long period encompasses different seasonal precipitation variations including wet and  
16 dry periods. The results show that the information retrieved from only a fraction of the  
17 discharge time series is relevant also for periods with very different characteristics.

18 Independently from the data quality issues, we also showed that the SDSA model performs  
19 better during the wet, winter periods than the dry, summer periods and dry years (see Sect.  
20 4.2). We interpret these results as an indication that the current model is not fully adapted to  
21 the high evapotranspiration conditions of our Mediterranean catchments. We must also point  
22 out that, when assessing the relevance of the estimated  $g(Q)$  function using continuous  
23 discharge simulations (Sect. 3.2), it is necessary to provide an estimate of *AET*. In this first  
24 approach, we used the hypothesis that  $AET=PET$  where *PET* is the rescaled  $K_C*ET_0$ . This  
25 assumption is crude because an average annual rescaling factor is used, whereas a monthly  
26 value would certainly be more relevant. The method of Thornthwaite and Mather (1955) cited  
27 by Gudulas et al. (2013) which provides monthly estimates of *AET* could be a way to improve  
28 our simulations in future works, and an example of application to the Ardèche at Meyras (#1)  
29 catchment is provided in Adamovic et al. (2015). Nevertheless, we show in Sect. 4.3 that  
30 rainfall retrieval during the vegetation period is poor, confirming the lower performance of the  
31 SDSA approach in this period. The method is therefore less reliable when discharge is low,  
32 especially in summer. This is one limitation of the SDSA for dry catchments.

1 In addition, the recent study of Brauer et al. (2013) showed that the two-parameter model they  
2 used, cannot deal with complexity of hydrological processes in their catchment (only 39 % of  
3 the hydrographs had *NSE* over 0.5). In the Ardèche catchments, the three-parameter model  
4 succeeds in capturing the catchment behavior, with quite good response of discharge to  
5 rainfall in low-vegetation periods (peaks and recession were nicely reproduced).

## 6 - interest of the SDSA approach as compared to other hydrological modelling 7 approaches

8 Recession analysis has been used to build hydrological models for many years (e.g. Brutsaert  
9 and Nieber, 1977). What is new in the SDSA approach is not the reservoir itself, but the  
10 manner to derive its structure and parameters from the data analysis: in particular, here the  
11 functional form of the storage-discharge relationship is not specified a priori, but determined  
12 directly from data without calibration (Kirchner, 2009). This is the very definition of the top-  
13 down or data-driven modelling approach, that is acknowledged to be a major paradigm shift  
14 in modelling by the hydrological community (and which was a major emphasis of the PUB  
15 decade; see, for instance, Sivapalan, 2003 and Hrachowitz et al., 2013). We argue that testing  
16 this kind of approach on new datasets, for various climatic conditions, contributes to the  
17 advance of hydrological science in itself. We have also compared the model results with other  
18 models that are based on similar data-driven methodology (e.g. Brauer et al., 2013 and  
19 Melsen et al., 2014) and obtained similar results.

20 The major limitation of the SDSA approach is of course the availability of good quality  
21 discharge data with a short time step, in catchments representative of the spatial variability of  
22 hydro-climatic conditions. Discharge must also be representative of natural conditions, which  
23 could also limit its applicability in catchments impacted by human activity.

## 24 5.2 Catchment functioning hypotheses derived from the analysis

25 The most important output from our application of the simple dynamical systems approach is  
26 the validation of underlying hypotheses and information about the dominant processes that  
27 can be derived from the model parameterization.

### 28 - General considerations

29 The SDSA model is based on an underlying hypothesis that regards a catchment as a single  
30 nonlinear bucket model. In our study we note the good performance of the model in each sub-  
31 catchment which suggests that SDSA, although it was developed for humid regions, remains

1 valid for these Mediterranean sub-catchments as well. We can thus interpret that these sub-  
2 catchments do follow the model's functioning hypotheses, especially in winter and low-  
3 vegetation periods. These results are consistent with the findings of Brauer et al. (2013) for  
4 the Hupsel Brook catchment, Kirchner (2009) for Plynlimon and Teuling et al. (2010) for the  
5 Rietholzbach catchment. In contrast, during the vegetation period the model seems to be less  
6 adapted to our Mediterranean setting. The catchments seem to behave differently when they  
7 are dry. This is probably due to the strong influence of evapotranspiration. In our  
8 hydroclimatic context (see details in next section), and taking into account that no regional  
9 groundwater exists in the Ardèche catchment, discharge provided by the SDSA approach can  
10 be associated with sub-surface flow (generally assumed to occur via lateral flow along  
11 perched water tables in shallow soils), which is less active in summer and when  
12 evapotranspiration is high. It could be necessary to consider another storage, probably more  
13 superficial than the "SDSA" storage, which could be used to supply evapotranspiration over  
14 shorter time scales, and which may be largely decoupled from sub-surface lateral flow that  
15 sustains base flows.

#### 16 - links with physiographic characteristics of the catchments

17 The model works better in the Ardèche at Meyras (#1) and Thines at Gournier Bridge (#3)  
18 catchments, which both are granitic (see Fig. 2). The hypothesis of shallow subsurface flow  
19 caused by saturation of at interface between soil and bedrock makes particular sense in this  
20 geology (e.g. Cosandey and Didon-Lescot, 1989; Trambly et al., 2010).

21 In the forested granitic catchments of this region, infiltration capacity is generally very high  
22 and runoff occurs due to soil saturation (e.g. Trambly et al., 2010). However, this saturation  
23 mostly occurs at the interface between the very thin soil and the large altered bedrock, where  
24 contrasts of hydraulic conductivity can be encountered, leading to quick lateral sub-surface  
25 flow. Experiments are currently being conducted on infiltration plots to quantify the velocity  
26 of this lateral flow (see Braud et al., 2014 for their description). Therefore the main  
27 mechanism we are speaking about is quick lateral sub-surface flow which transits through the  
28 reservoir considered in the Simple Dynamical System Approach. On agricultural areas, in the  
29 intermediate part of the Ardèche catchment, infiltration excess surface runoff is likely to  
30 occur (and has been observed in the field). Its contribution is also under investigation using  
31 detailed experiments (see Braud et al., 2014).

32 In addition, unaltered bedrock tends to be impermeable, but flow pathways are created in the  
33 many fractures, joints and fissures of the altered horizons. During extended rainfall those flow

1 pathways might become connected, generating rapid subsurface flow (Krier et al., 2012).  
2 Moreover the parameter values of the granite catchments are quite similar (see Table 6).

3 To quantify the relative influence of several predictors of the catchment response (and values  
4 of  $C_1$ ,  $C_2$ ,  $C_3$  parameters), Adamovic (2014) used Factor Analysis of Mixed Data (FAMD).  
5 By using this statistical technique along with HCPC (Hierarchical Clustering on Principal  
6 Components) analysis, geology was found to be the only dominant predictor of runoff  
7 variability. The role of geology is more thoroughly demonstrated in Adamovic (2014) for the  
8 catchments studied in this paper and in Coussot (2015) for a larger set of catchments from the  
9 Cévennes region, but a review of this work is beyond the scope of the present paper.

10 This is also consistent with the contemporary literature, as geology has been invoked in  
11 numerous recent studies as a controlling factor of flood response (Gaál et al., 2012;  
12 Garambois et al., 2013; Krier et al., 2012; Vannier et al., 2013). As also discussed by Kirchner  
13 (2009), the theory is challenged by catchments with heterogeneous geology and thus with  
14 many disconnected subsurface storage reservoirs. This might explain the good modeling  
15 performance in granite catchments (see also Vannier, 2013 for similar conclusions using a  
16 reductionist modeling approach).

17

## 18 **6 Conclusion and perspectives**

19 Our study describes in detail the application of Kirchner's methodology to four catchments of  
20 the Ardèche basin ranging from 16 to 103 km<sup>2</sup>, typical of the **Western** Mediterranean  
21 environment.

22 To have more representative water balance fluxes, we rescaled precipitation and  
23 evapotranspiration for three sub-catchments (#2, #3 and #4). In our work we used average  
24 annual scaling coefficients for the whole time series (for both precipitation and  
25 evapotranspiration). In the future, varying these scaling coefficients according to different  
26 seasons could possibly lead to a better approximation of hourly precipitation and  
27 evapotranspiration fluxes.

28 We calculated the discharge sensitivity functions from low-vegetation periods and performed  
29 continuous discharge simulations with an hourly time step for the period 2000-2008. We also  
30 inferred precipitation and performed sensitivity analyses of the three parameters of the  
31 discharge sensitivity function.

1 Our results show that good results for discharge simulation can be obtained, especially under  
2 winter humid conditions and for catchments characterized by predominantly granitic  
3 lithology. Under dry conditions, poor model performance is mainly related to the disturbed  
4 water balance terms, high influence of *AET* and imprecise discharge measurements.  
5 Improving *AET* estimation is recommended for better model performance in summer periods  
6 when evapotranspiration is high and when the unsaturated zone has a significant role in  
7 attenuating the precipitation input. Working on the quantification of data accuracy and error  
8 reduction is also recommended in order to get more robust and reliable results.

9 As a perspective to this study, dominant predictors of runoff variability other than geology  
10 (such as land use, soil properties, drainage density, topographic steepness etc.) still need to be  
11 explored and linked to catchment hydrological behavior. Relating the obtained parameters of  
12 the discharge sensitivity function to the catchment characteristics using different statistical  
13 classification techniques (e.g. Principal Component Analysis (PCA) and Factor Analysis of  
14 Mixed Data (FAMD) or Self-Organized Maps) could allow us to apply the method also to  
15 ungauged basins, thus contributing to the PUB initiative (Hrachowitz et al., 2013). Another  
16 step would be then to create a distributed “Kirchner type” hydrological model where a  
17 parameter set would be attributed to “regions” discretized on the basis of their physiographic  
18 characteristics. This would allow us to determine the rainfall-runoff behavior in large scale  
19 river basins by taking into account the precipitation spatial distribution and flood flow routing  
20 through the channel network. We would then be able to broaden our understanding of non-  
21 linear catchment response and travel time lags as suggested by Kirchner (2009).

22

## 23 **Acknowledgments**

24 The study is conducted within the FloodScale project, funded by the French National  
25 Research Agency (ANR) under contract n° ANR 2011 BS56 027, which contributes to the  
26 HyMeX program. The HyMeX database teams (ESPRI/IPSL and SEDOO/Observatoire Midi-  
27 Pyrénées) helped in accessing the data. The authors acknowledge Brice Boudevillain for  
28 providing the OHM-CV rainfall data, Météo-France for their rainfall and SAFRAN climate  
29 data. EdF-DTG provided discharge data from three of the gauges used in this study. We thank  
30 the Region Rhône-Alpes for its funding of the PhD grant of the first author. We thank R.  
31 Krier for providing us the codes used to perform the recession analysis and E. Leblois for  
32 constructive comments on the paper.

33

## 1 **References**

2

3 Adamovic, M.: Development of a data-driven distributed hydrological model for regional  
4 catchments prone to Mediterranean flash floods. Application to the Ardèche catchment  
5 (France). PhD thesis, University of Grenoble, France, 2014.

6 Adamovic, M. et al.: Interactive comment on “Does the simple dynamical systems approach  
7 provide useful information about catchment hydrological functioning in a Mediterranean  
8 context? Application to the Ardèche catchment (France)” by M. Adamovic et al., *Hydrol.*  
9 *Earth Syst. Sci. Discuss.*, 11, C6170–C6171, 2015.

10 Allen, R., Pereira, L., Raes, D., and Smith, M.: Crop evapotranspiration - Guidelines for  
11 computing crop water requirements - FAO Irrigation and drainage paper 56, citeulike-article-  
12 id:10458368, 1998.

13 Beven, K., and Binley, A.: The future of distributed models: Model calibration and uncertainty  
14 prediction, *Hydrological Processes*, 6, 279-298, 10.1002/hyp.3360060305, 1992.

15 Beven, K.: Towards a coherent philosophy for modelling the environment, *Proceedings of the*  
16 *Royal Society of London. Series A: Mathematical, Physical and Engineering Sciences*, 458,  
17 2465-2484, 10.1098/rspa.2002.0986, 2002.

18 Blöschl, G., and Sivapalan, M.: Scale issues in hydrological modelling: a review,  
19 *Hydrological Processes*, 9, 251-290, 1995.

20 Bonnifait, L., Delrieu, G., Lay, M. L., Boudevillain, B., Masson, A., Belleudy, P., Gaume, E.,  
21 and Saulnier, G.-M.: Distributed hydrologic and hydraulic modelling with radar rainfall input:  
22 Reconstruction of the 8–9 September 2002 catastrophic flood event in the Gard region,  
23 France, *Advances in Water Resources*, 32, 1077-1089,  
24 <http://dx.doi.org/10.1016/j.advwatres.2009.03.007>, 2009.

25 Boronina, A., Golubev, S., and Balderer, W.: Estimation of actual evapotranspiration from an  
26 alluvial aquifer of the Kouris catchment (Cyprus) using continuous streamflow records,  
27 *Hydrological Processes*, 19, 4055-4068, 2005.

28 Boudevillain, B., Delrieu, G., Galabertier, B., Bonnifait, L., Bouilloud, L., Kirstetter, P.-E.,  
29 and Mosini, M.-L.: The Cévennes-Vivarais Mediterranean Hydrometeorological Observatory  
30 database, *Water Resources Research*, 47, W07701, 10.1029/2010wr010353, 2011.



1 Branger, F., Dramais, G., Horner, I., Le Boursicaud, R., Le Coz, J., and Renard, B. :  
2 Improving the quantification of flash flood hydrographs and reducing their uncertainty using  
3 noncontact streamgauging methods, EGU General Assembly 2015, Vienna, 12-17 April 2015,  
4 Geophysical Research Abstracts, Vol. 17, EGU2015-5768, 2015.

5 Braud, I., Roux, H., Anquetin, S., Maubourguet, M.-M., Manus, C., Viallet, P., and Dartus, D.:  
6 The use of distributed hydrological models for the Gard 2002 flash flood event: Analysis of  
7 associated hydrological processes, Journal of Hydrology, 394, 162-181,  
8 <http://dx.doi.org/10.1016/j.jhydrol.2010.03.033>, 2010.

9 Braud, I., Ayral, P. A., Bouvier, C., Branger, F., Delrieu, G., Le Coz, J., Nord, G.,  
10 Vandervaere, J. P., Anquetin, S., Adamovic, M., Andrieu, J., Batiot, C., Boudevillain, B.,  
11 Brunet, P., Carreau, J., Confoland, A., Didon-Lescot, J. F., Domergue, J. M., Douvinet, J.,  
12 Dramais, G., Freydier, R., Gérard, S., Huza, J., Leblois, E., Le Bourgeois, O., Le Boursicaud,  
13 R., Marchand, P., Martin, P., Nottale, L., Patris, N., Renard, B., Seidel, J. L., Taupin, J. D.,  
14 Vannier, O., Vincendon, B., and Wijbrans, A.: Multi-scale hydrometeorological observation  
15 and modelling for flash-flood understanding, Hydrol. Earth Syst. Sci. 11, 1871-1945,  
16 [10.5194/hessd-11-1871-2014](https://doi.org/10.5194/hessd-11-1871-2014), 2014.

17 Brauer, C. C., Teuling, A. J., Torfs, P. J. J. F., and Uijlenhoet, R.: Investigating storage-  
18 discharge relations in a lowland catchment using hydrograph fitting, recession analysis, and  
19 soil moisture data, Water Resources Research, 49, 4257-4264, [10.1002/wrcr.20320](https://doi.org/10.1002/wrcr.20320), 2013.

20 Brutsaert, W., and Nieber, J. L.: Regionalized drought flow hydrographs from a mature  
21 glaciated plateau, Water Resources Research, 13, 637-643, [10.1029/WR013i003p00637](https://doi.org/10.1029/WR013i003p00637),  
22 1977.

23 Budyko, M. I.: Climate and life, English Edition edited by Miller, D. H., Academic Press, 508  
24 pp., 1974.

25 Cosandey, C., and Didon-Lescot, J. F.: Etude des crues cevenoles: conditions d'apparition  
26 dans un petit bassin forestier sur le versant sud du Mont Lozere, France, International  
27 Association of Hydrological Sciences, Wallingford, ROYAUME-UNI, 13 pp., 1989.

28 Coussot, C.: Assessing and modelling hydrological behaviours of Mediterranean catchments  
29 using discharge recession analysis. Master Thesis, HydroHazards, University of Grenoble,  
30 France, 54 pp., 2015.

1 Delrieu, G., Wijbrans, A., Boudevillain, B., Faure, D., Bonnifait, L., and Kirstetter, P.-E.:  
2 Geostatistical radar–raingauge merging: A novel method for the quantification of rain  
3 estimation accuracy, *Advances in Water Resources*, 71, 110-124,  
4 <http://dx.doi.org/10.1016/j.advwatres.2014.06.005>, 2014.

5 Drobinski, P., Ducrocq, V., Alpert, P., Anagnostou, E., Béranger, K., Borga, M., Braud, I.,  
6 Chanzy, A., Davolio, S., Delrieu, G., Estournel, C., Boubrahmi, N. F., Font, J., Grubisic, V.,  
7 Gualdi, S., Homar, V., Ivancan-Picek, B., Kottmeier, C., Kotroni, V., Lagouvardos, K.,  
8 Lionello, P., Llasat, M. C., Ludwig, W., Lutoff, C., Mariotti, A., Richard, E., Romero, R.,  
9 Rotunno, R., Roussot, O., Ruin, I., Somot, S., Taupier-Letage, I., Tintore, J., Uijlenhoet, R.,  
10 and Wernli, H.: HyMeX, a 10-year multidisciplinary program on the Mediterranean water  
11 cycle, *Bulletin of the American Meteorological Society*, 10.1175/BAMS-D-12-00242.1, 2013.

12 Duband, D., Obled, C., and Rodriguez, J. Y.: Unit hydrograph revisited: an alternate iterative  
13 approach to UH and effective precipitation identification, *Journal of Hydrology*, 150, 115-149,  
14 [http://dx.doi.org/10.1016/0022-1694\(93\)90158-6](http://dx.doi.org/10.1016/0022-1694(93)90158-6), 1993.

15 Etchevers, P., Durand, Y., Habets, F., Martin, E., and Noilhan, J.: Impact of spatial resolution  
16 on the hydrological simulation of the Durance high-Alpine catchment, France, *Annals of  
17 Glaciology*, 32, 87-92, 2001.

18 Freeze, R. A., and Harlan, R. L.: Blueprint for a physically-based, digitally-simulated  
19 hydrologic response model, *Journal of Hydrology*, 9, 237-258,  
20 [http://dx.doi.org/10.1016/0022-1694\(69\)90020-1](http://dx.doi.org/10.1016/0022-1694(69)90020-1), 1969.

21 Fu, B. P.: On the calculation of the evaporation from land surface (in Chinese), *Sci. Atmos.  
22 Sin.*, 5, 23-31, 1981.

23 Gaál, L., Szolgay, J., Kohnová, S., Parajka, J., Merz, R., Viglione, A., and Blöschl, G.: Flood  
24 timescales: Understanding the interplay of climate and catchment processes through  
25 comparative hydrology, *Water Resources Research*, 48, W04511, 10.1029/2011WR011509,  
26 2012.

27 Gao, Z. Q., Liu, C. S., Gao, W., and Chang, N. B.: A coupled remote sensing and the Surface  
28 Energy Balance with Topography Algorithm (SEBTA) to estimate actual evapotranspiration  
29 over heterogeneous terrain, *Hydrol. Earth Syst. Sci.*, 15, 119-139, 10.5194/hess-15-119-2011,  
30 2011.

1 Garambois, P. A., Roux, H., Larnier, K., Castaings, W., and Dartus, D.: Characterization of  
2 process-oriented hydrologic model behavior with temporal sensitivity analysis for flash floods  
3 in Mediterranean catchments, *Hydrol. Earth Syst. Sci.*, 17, 2305-2322, 10.5194/hess-17-2305-  
4 2013, 2013.

5 Gaume, E., Bain, V., Bernardara, P., Newinger, O., Barbuc, M., Bateman, A., Blaškovičová,  
6 L., Blöschl, G., Borga, M., Dumitrescu, A., Daliakopoulos, I., Garcia, J., Irimescu, A.,  
7 Kohnova, S., Koutroulis, A., Marchi, L., Matreata, S., Medina, V., Preciso, E., Sempere-  
8 Torres, D., Stancalie, G., Szolgay, J., Tsanis, I., Velasco, D., and Viglione, A.: A compilation  
9 of data on European flash floods, *Journal of Hydrology*, 367, 70-78,  
10 <http://dx.doi.org/10.1016/j.jhydrol.2008.12.028>, 2009.

11 Gottardi, F.: Estimation statistique et reanalyse des precipitations en montagne - Utilisation  
12 d'ébauches par types de temps et assimilation de donnees d'enneigement : Application aux  
13 grands massifs montagneux francais, *Hydrology*, Institut Polytechnique de Grenoble-INPG,  
14 French, <https://tel.archives-ouvertes.fr/>, 261 pp, 2009.

15 Gudulas, K., Voudouris, K., Soulios, G., and Dimopoulos, G.: Comparison of different  
16 methods to estimate actual evapotranspiration and hydrologic balance, *Desalination and*  
17 *Water Treatment*, 51, 2945-2954, 10.1080/19443994.2012.748443, 2013.

18 Gupta, H. V., Sorooshian, S., and Yapo, P. O.: Status of automatic calibration for hydrologic  
19 models: Comparison with multilevel expert calibration, *Journal of Hydrologic Engineering*, 4,  
20 135-143, 1999.

21 Hernández, E., Cana, L., Díaz, J., García, R., and Gimeno, L.: Mesoscale convective  
22 complexes over the western Mediterranean area during 1990-1994, *Meteorol. Atmos. Phys.*, 68,  
23 1-12, 1998.

24 Hrachowitz, M., Savenije, H. H. G., Blöschl, G., McDonnell, J. J., Sivapalan, M., Pomeroy, J.  
25 W., Arheimer, B., Blume, T., Clark, M. P., Ehret, U., Fenicia, F., Freer, J. E., Gelfan, A.,  
26 Gupta, H. V., Hughes, D. A., Hut, R. W., Montanari, A., Pande, S., Tetzlaff, D., Troch, P. A.,  
27 Uhlenbrook, S., Wagener, T., Winsemius, H. C., Woods, R. A., Zehe, E., and Cudennec, C.: A  
28 decade of Predictions in Ungauged Basins (PUB)—a review, *Hydrological Sciences Journal*,  
29 58, 1198-1255, 10.1080/02626667.2013.803183, 2013.

30 Kirchner, J. W.: Getting the right answers for the right reasons: Linking measurements,  
31 analyses, and models to advance the science of hydrology, *Water Resources Research*, 42,  
32 W03S04, 10.1029/2005wr004362, 2006.

1 Kirchner, J. W.: Catchments as simple dynamical systems: Catchment characterization,  
2 rainfall-runoff modeling, and doing hydrology backward, *Water Resources Research*, 45,  
3 W02429, [10.1029/2008WR006912](https://doi.org/10.1029/2008WR006912), 2009.

4 Klemes, V.: Operational testing of hydrological simulation models, *Hydrological Sciences*  
5 *Journal/Journal des Sciences Hydrologiques*, 31, 13-24, 1986.

6 Klemeš, V.: Conceptualization and scale in hydrology, *Journal of Hydrology*, 65, 1-23,  
7 [http://dx.doi.org/10.1016/0022-1694\(83\)90208-1](http://dx.doi.org/10.1016/0022-1694(83)90208-1), 1983.

8 Krier, R., Matgen, P., Goergen, K., Pfister, L., Hoffmann, L., Kirchner, J. W., Uhlenbrook, S.,  
9 and Savenije, H. H. G.: Inferring catchment precipitation by doing hydrology backward: A  
10 test in 24 small and mesoscale catchments in Luxembourg, *Water Resources Research*, 48,  
11 W10525, [10.1029/2011WR010657](https://doi.org/10.1029/2011WR010657) 2012.

12 Lafaysse, M., Hingray, B., Etchevers, P., Martin, E., and Obled, C.: Influence of spatial  
13 discretization, underground water storage and glacier melt on a physically-based hydrological  
14 model of the Upper Durance River basin, *Journal of Hydrology*, 403, 116-129, 2011.

15 Lang, M., Moussay, D., Recking, A., and Naulet, R.: Hydraulic modelling of historical floods:  
16 a case study on the Ardeche river at Vallon-Pont-d'Arc, 183-189, 2002.

17 Le Coz, J., Hauet, A., Pierrefeu, G., Dramais, G., and Camenen, B.: Performance of image-  
18 based velocimetry (LSPIV) applied to flash-flood discharge measurements in Mediterranean  
19 rivers, *Journal of Hydrology*, 394, 42-52, <http://dx.doi.org/10.1016/j.jhydrol.2010.05.049>,  
20 2010.

21 Le Coz, J., Renard, B., Bonnifait, L., Branger, F., and Le Boursicaud, R.: Combining  
22 hydraulic knowledge and uncertain gaugings in the estimation of hydrometric rating curves: A  
23 Bayesian approach, *Journal of Hydrology*, 509, 573-587,  
24 <http://dx.doi.org/10.1016/j.jhydrol.2013.11.016>, 2014.

25 Le Lay, M., and Saulnier, G. M.: Exploring the signature of climate and landscape spatial  
26 variabilities in flash flood events: Case of the 8–9 September 2002 Cévennes-Vivarais  
27 catastrophic event, *Geophysical Research Letters*, 34, L13401, [10.1029/2007GL029746](https://doi.org/10.1029/2007GL029746),  
28 2007.

29 Manus, C., Anquetin, S., Braud, I., Vandervaere, J. P., Creutin, J. D., Viallet, P., and Gaume,  
30 E.: A modeling approach to assess the hydrological response of small mediterranean

1 catchments to the variability of soil characteristics in a context of extreme events, *Hydrol.*  
2 *Earth Syst. Sci.*, 13, 79-97, 10.5194/hess-13-79-2009, 2009.

3 McDonnell, J. J., Sivapalan, M., Vaché, K., Dunn, S., Grant, G., Haggerty, R., Hinz, C.,  
4 Hooper, R., Kirchner, J., Roderick, M. L., Selker, J., and Weiler, M.: Moving beyond  
5 heterogeneity and process complexity: A new vision for watershed hydrology, *Water*  
6 *Resources Research*, 43, W07301, 10.1029/2006WR005467, 2007.

7 Melsen, L. A., Teuling, A. J., van Berkum, S. W., Torfs, P. J. J. F., and Uijlenhoet, R.:  
8 Catchments as simple dynamical systems: A case study on methods and data requirements for  
9 parameter identification, *Water Resources Research*, 50, 5577-5596,  
10 10.1002/2013WR014720, 2014.

11 Molinié, G., Ceresetti, D., Anquetin, S., Creutin, J. D., and Boudevillain, B.: Rainfall Regime  
12 of a Mountainous Mediterranean Region: Statistical Analysis at Short Time Steps, *Journal of*  
13 *Applied Meteorology and Climatology*, 51, 429-448, 10.1175/2011JAMC2691.1, 2011.

14 Moriasi, D. N., Arnold, J. G., Van Liew, M. W., Bingner, R. L., Harmel, R. D., and Veith, T.  
15 L.: Model evaluation guidelines for systematic quantification of accuracy in watershed  
16 simulations, *Transactions of the ASABE*, 50, 885-900, 2007.

17 Nash, J. E., and Sutcliffe, J. V.: River flow forecasting through conceptual models part I - A  
18 discussion of principles, *Journal of Hydrology*, 10, 282-290, 1970.

19 Naulet, R., Lang, M., Ouarda, T. B. M. J., Coeur, D., Bobée, B., Recking, A., and Moussay,  
20 D.: Flood frequency analysis on the Ardèche river using French documentary sources from  
21 the last two centuries, *Journal of Hydrology*, 313, 58-78, 2005.

22 Pike, J. G.: The estimation of annual run-off from meteorological data in a tropical climate,  
23 *Journal of Hydrology*, 2, 116-123, [http://dx.doi.org/10.1016/0022-1694\(64\)90022-8](http://dx.doi.org/10.1016/0022-1694(64)90022-8), 1964.

24 Quintana-Seguí, P., Le Moigne, P., Durand, Y., Martin, E., Habets, F., Baillon, M., Canellas,  
25 C., Franchisteguy, L., and Morel, S.: Analysis of near-surface atmospheric variables:  
26 Validation of the SAFRAN analysis over France, *Journal of Applied Meteorology and*  
27 *Climatology*, 47, 92-107, 2008.

28 Reggiani, P., Sivapalan, M., and Majid Hassanizadeh, S.: A unifying framework for watershed  
29 thermodynamics: balance equations for mass, momentum, energy and entropy, and the second  
30 law of thermodynamics, *Advances in Water Resources*, 22, 367-398,  
31 [http://dx.doi.org/10.1016/S0309-1708\(98\)00012-8](http://dx.doi.org/10.1016/S0309-1708(98)00012-8), 1998.

1 Samaniego, L., Kumar, R., and Attinger, S.: Multiscale parameter regionalization of a grid-  
2 based hydrologic model at the mesoscale, *Water Resources Research*, 46, W05523,  
3 10.1029/2008WR007327, 2010.

4 Saulnier, G. M., and Le Lay, M.: Sensitivity of flash-flood simulations on the volume, the  
5 intensity, and the localization of rainfall in the Cévennes-Vivarais region (France), *Water*  
6 *Resources Research*, 45, W10425, 10.1029/2008WR006906, 2009.

7 Schreiber, P.: Über die Beziehungen zwischen dem Niederschlag und der Wasserführung der  
8 Flüsse in Mitteleuropa, *Zeitschrift für Meteorologie*, 21, 441-452, 1904.

9 Seiler, C., and Moene, A. F.: Estimating Actual Evapotranspiration from Satellite and  
10 Meteorological Data in Central Bolivia, *Earth Interactions*, 15, 1-24, 10.1175/2010EI332.1,  
11 2010.

12 Sempere-Torres, D., Rodriguez-Hernandez, J. Y., and Obled, C.: Using the DPFT approach to  
13 improve flash flood forecasting models, *Natural Hazards*, 5, 17-41, 1992.

14 Sheffer, N. A., Enzel, Y., and Benito, G.: Paleofloods in southern France-the Ardeche River,  
15 PHEFRA workshop, Barcelona, 25-31, 2002.

16 Sivapalan, M.: Process complexity at hillslope scale, process simplicity at the watershed  
17 scale: is there a connection?, *Hydrological Processes*, 17, 1037-1041, 10.1002/hyp.5109,  
18 2003a.

19 Sivapalan, M.: Prediction in ungauged basins: a grand challenge for theoretical hydrology,  
20 *Hydrological Processes*, 17, 3163-3170, 10.1002/hyp.5155, 2003b.

21 Sivapalan, M.: Pattern, Process and Function: Elements of a Unified Theory of Hydrology at  
22 the Catchment Scale, in: *Encyclopedia of Hydrological Sciences*, John Wiley & Sons, Ltd,  
23 Chichester, UK, 193–219, DOI: 10.1002/0470848944.hsa012, 2006.

24 Tarboton, D. G., Schreuders, K. A. T., Watson, D. W., and Baker, M. E.: Generalized terrain-  
25 based flow analysis of digital elevation models, 18th World IMACS Congress and  
26 MODSIM09 International Congress on Modelling and Simulation, 2000-2006, 2009.

27 Tekleab, S., Uhlenbrook, S., Mohamed, Y., Savenije, H. H. G., Temesgen, M., and Wenninger,  
28 J.: Water balance modeling of Upper Blue Nile catchments using a top-down approach,  
29 *Hydrology and Earth System Sciences*, 15, 2179-2193, 2011.

1 Teuling, A. J., Lehner, I., Kirchner, J. W., and Seneviratne, S. I.: Catchments as simple  
2 dynamical systems: Experience from a Swiss prealpine catchment, *Water Resources Research*,  
3 46, W10502, 10.1029/2009WR008777, 2010.

4 Thierion, C., Longuevergne, L., Habets, F., Ledoux, E., Ackerer, P., Majdalani, S., Leblois, E.,  
5 Lecluse, S., Martin, E., Queguiner, S., and Viennot, P.: Assessing the water balance of the  
6 Upper Rhine Graben hydrosystem, *Journal of Hydrology*, 424–425, 68–83,  
7 <http://dx.doi.org/10.1016/j.jhydrol.2011.12.028>, 2012.

8 **Thornthwaite, C. and Mather, J., The water balance, *Climatology*, VIII (I), New-Jersey, NY,**  
9 **1-37, 1955.**

10 Tognetti, S. S., Aylward, B., and Mendoza, G. F.: Markets for Watershed Services, in:  
11 *Encyclopedia of Hydrological Sciences*, John Wiley & Sons, Ltd, UK, 2987-3002,  
12 DOI: 10.1002/0470848944.hsa202, 2006.

13 Trambly Y., Bouvier C., Crespy A., Marchandise A., 2010. Improvement of flash flood  
14 modelling using spatial patterns of rainfall: a case study in south of France. *Global Change:*  
15 *Facing Risks and Threats to Water Resources (Proceedings of the Sixth World FRIEND*  
16 *Conference, Fez, Morocco, October 2010). IAHS Publ. 340, 172-178,*  
17 <http://y.trambly.free.fr/doc/Trambly-redbook.340.pdf>, 2010.

18 **Turc, L.: Nouvelles formules pour le bilan d'eau en fonction des valeurs moyennes annuelles**  
19 **de précipitations et de la température, *Comptes Rendus de l'Académie des Sciences, Paris,***  
20 **233, 633-635, 1951.**

21 Uhlenbrook, S., Seibert, J. A. N., Leibundgut, C., and Rodhe, A.: Prediction uncertainty of  
22 conceptual rainfall-runoff models caused by problems in identifying model parameters and  
23 structure, *Hydrological Sciences Journal*, 44, 779-797, 10.1080/02626669909492273, 1999.

24 Vannier, O.: Apport de la modélisation hydrologique régionale à la compréhension des  
25 processus de crue en zone méditerranéenne, Thèse de l'Ecole doctorale Terre, Univers,  
26 Environnement, University of Grenoble, Grenoble, France, 22 Novembre 2013, 274 pp.,  
27 2013.

28 Vannier, O., Braud, I., and Anquetin, S.: Regional estimation of catchment-scale soil  
29 properties by means of streamflow recession analysis for use in distributed hydrological  
30 models, *Hydrological Processes*, 28, 6276-6291, 10.1002/hyp.10101, 2014.

1 Vidal, J. P., Martin, E., Franchistéguy, L., Baillon, M., and Soubeyroux, J. M.: A 50-year high-  
2 resolution atmospheric reanalysis over France with the Safran system, *International Journal of*  
3 *Climatology*, 30, 1627-1644, 2010.

4 Yan, Z., Gottschalk, L., Leblois, E., and Xia, J.: Joint mapping of water balance components  
5 in a large Chinese basin, *Journal of Hydrology*, 450–451, 59-69,  
6 <http://dx.doi.org/10.1016/j.jhydrol.2012.05.030>, 2012.

7 Zehe, E., Lee, H., and Sivapalan, M.: Dynamical process upscaling for deriving catchment  
8 scale state variables and constitutive relations for meso-scale process models, *Hydrology and*  
9 *Earth System Sciences*, 10, 981-996, 2006.

10 Zhang, L., Hickel, K., Dawes, W. R., Chiew, F. H. S., Western, A. W., and Briggs, P. R.: A  
11 rational function approach for estimating mean annual evapotranspiration, *Water Resources*  
12 *Research*, 40, W02502, [10.1029/2003WR002710](https://doi.org/10.1029/2003WR002710), 2004.

13 Zhang, L., Potter, N., Hickel, K., Zhang, Y., and Shao, Q.: Water balance modeling over  
14 variable time scales based on the Budyko framework - Model development and testing,  
15 *Journal of Hydrology*, 360, 117-131, 2008.

16 Wittenberg, H., and Sivapalan, M.: Watershed groundwater balance estimation using  
17 streamflow recession analysis and baseflow separation, *Journal of Hydrology*, 219, 20-33,  
18 [10.1016/S0022-1694\(99\)00040-2](https://doi.org/10.1016/S0022-1694(99)00040-2), 1999.

19  
20  
21  
22  
23  
24  
25  
26  
27  
28



1 Table 1. Physiographic characteristics of the four examined Ardèche sub-catchments. Strahler  
 2 stream order, channel length and drainage density are calculated from the 25 m IGN DTM  
 3 using TauDEM tools (Tarboton et al., 2009)

Catchment ID	#1	#2	#3	#4
River and catchment name	Ardèche at Meyras	Borne at Nicolaud Bridge	Thines at Gournier Bridge	Altier at Goulette
River name	Ardèche	Borne	Thines	Altier
Drainage area (km <sup>2</sup> ), A	98.43	62.6	16.73	103.42
Average altitude (m)	898.54	1113	892.75	1149.13
Average slope (%)	23.43	20.13	16.72	17.13
Forest cover (%)	68	68	51	42
Strahler stream order	4	3	3	5
Channel length (km), L	94.31	59.26	13.51	97.38
Drainage density (km/km <sup>2</sup> ), D=L/A	0.96	0.95	0.81	0.94

4

5 Table 2. Weighted average crop coefficient for each examined catchment per growing stage

Catchment name	$K_c$ initial (Jan.-Apr.)	$K_c$ mid_season (May-Oct.)	$K_c$ late_season (Nov.-Dec.)
The Ardèche at Meyras (#1)	0.74	0.94	0.79
Borne at Nicolaud Bridge (#2)	0.73	0.96	0.80
Thines at Gournier Bridge (#3)	0.68	0.94	0.75
Altier at Goulette (#4)	0.62	0.97	0.75

6

7

8

9

10

11

12

13

1 Table 3. Hydro-climatic characteristics of the four examined Ardèche sub-catchments (2000-  
2 2008).

Catchment ID	#1	#2	#3	#4
Catchment name	Ardèche at Meyras	Borne at Nicolaud Bridge	Thines at Gournier Bridge	Altier at Goulette
Precipitation (mm yr <sup>-1</sup> ), $P$	1621	1633	1892	1176
Streamflow (mm yr <sup>-1</sup> ), $Q$	1057	1579	970	932
Runoff coefficient, $C$	0.65	0.97	0.51	0.79
Actual Evapotranspiration (mm yr <sup>-1</sup> ), $AET_{wb}=P-Q$	564	54	922	244
$ET_0$ SAFRAN (mm yr <sup>-1</sup> )	809	792	860	775
$K_c ET_0$ (mm yr <sup>-1</sup> )	731	729	762	699

3 Table 4. Scaling hydro-climatic characteristics of the four examined Ardèche sub-catchments  
4 (2000-2008).

Catchment ID	#1	#2	#3	#4
Catchment name	Ardèche at Meyras	Borne at Nicolaud Bridge	Thines at Gournier Bridge	Altier at Goulette
Turc Actual evapotranspiration (mm yr <sup>-1</sup> ), $AET_{Turc}$	609	505	571	475
Runoff coefficient, $C_{Turc}$	0.62	0.69	0.70	0.60
Temperature (°C), $T$	11.2	8.0	9.9	7.7
$P_{Turc}$ (mm yr <sup>-1</sup> )	-	2084	1541	1407
Scaling $P$ coefficient, $\alpha_p$	-	1.27	0.81	1.2
Scaling $AET$ coefficient, $\alpha_{AET}$	-	0.69	0.75	0.68
New runoff coefficient, $C_n$	0.65	0.76	0.63	0.66

5  
6  
7  
8  
9  
10  
11  
12

1 Table 5. Description of different empirical formulas for estimating mean annual actual  
 2 evapotranspiration ( $AET$  is actual evapotranspiration ( $\text{mm yr}^{-1}$ ),  $P$  is precipitation ( $\text{mm yr}^{-1}$ ),  
 3  $ET_0$  is potential evapotranspiration ( $\text{mm yr}^{-1}$ ), and  $T$  is mean air temperature ( $^{\circ}\text{C}$ )).

Equation	Reference
$AET = P[1 - \exp(-\frac{ET_0}{P})]$	(Schreiber, 1904)
$AET = \frac{P}{\sqrt{0.9 + (\frac{P}{L})^2}} \text{ where } L = 300 + 25T + 0.05T^3$	(Turc, 1951)
$AET = P / \left[ 1 + \left( \frac{P}{ET_0} \right)^2 \right]^{0.5}$	(Pike, 1964)
$AET = \left[ P \left( 1 - \exp\left(-\frac{ET_0}{P}\right) \right) ET_0 \tanh\left(\frac{P}{ET_0}\right) \right]^{0.5}$	(Budyko, 1974)

4

5 Table 6. Parameter values for the examined catchments for all low-vegetation periods (2000-  
 6 2008).

Catchment name (ID)	$C_1$	$C_2$	$C_3$
The Ardèche at Meyras (#1)	-3.74	0.65	-0.2
Borne at Nicolaud Bridge (#2)	-4.08	0.74	-0.15
Thines at Gournier Bridge (#3)	-3.71	0.72	-0.13
Altier at Goulette (#4)	-3.80	0.82	-0.02

7

8

9

10

11

12

13

14

15

16

1 Table 7. Summary statistics of computed *NSE*, *NSE log* and *PBIAS* for each examined  
 2 catchment in the Ardèche basin.

Year	The Ardèche at Meyras (#1)			Borne at Nicolaud Bridge (#2)			Thines at Gournier Bridge (#3)			Altier at Goulette (#4)		
	NSE linear	NSE log	PBIAS (%)	NSE linear	NSE log	PBIAS (%)	NSE linear	NSE log	PBIAS (%)	NSE linear	NSE log	PBIAS (%)
2000	0.60	0.85	-20.7	0.76	0.83	5.02	0.49	0.86	-18.14	0.53	0.70	-1.58
2001	0.61	0.85	5.7	0.59	0.74	33.56	0.27	0.85	-1.43	0.67	0.62	1.86
2002	0.82	0.82	-1.2	0.63	0.53	-12.77	0.68	0.83	-15.05	0.65	0.44	-17.88
2003	0.76	0.72	13.	0.73	0.63	5.78	0.79	0.82	14.27	0.89	-0.19	12.43
2004	0.69	0.86	5.1	-0.07	0.37	-35.28	-0.26	0.78	-18.38	0.42	0.05	-11.09
2005	-0.15	0.07	62.2	0.66	0.64	18.16	0.21	0.53	48.22	0.70	-0.86	0.04
2006	0.51	0.71	19.6	0.68	0.58	0.58	0.36	0.72	17.67	0.18	-0.61	6.90
2007	0.11	0.67	21.8	0.51	0.28	-23.67	0.30	0.71	24.47	-1.22	0.34	-14.48
2008	0.76	0.85	8.2	0.75	0.43	-9.35	0.69	0.79	-6.89	0.83	0.62	6.04
2000-2008	0.68	0.74	7.9	0.67	0.61	0.75	0.55	0.78	0.98	0.74	0.18	-0.29

3

4 Table 8. Model performance of inferred versus measured daily rainfall in four sub-catchments  
 5 for all low-vegetation periods 2000-2008.

Gauging station	$R^2$	Mean Bias (mm day <sup>-1</sup> )	Slope	Time lag (hour)
Ardèche at Meyras (#1)	0.41	7.9	1.1	2 (optimized)
Ardèche at Meyras (#1)	0.41	7.9	1.1	1
Borne at Nicolaud Bridge (#2)	0.56	7.4	1.01	2 (optimized)
Thines at Gournier Bridge (#3)	0.61	4.7	1.22	2 (optimized)
Altier at Goulette (#4)	0.71	2	1.09	2
Altier at Goulette (#4)	0.72	2	1.09	1 (optimized)

6

7

8

9

10

11

12

13

1 Table 9. *NSE* values of log discharge for the Ardèche at Meyras (#1) catchment, illustrating  
 2 sensitivity to changes in the  $C_1$  and  $C_3$  parameters.

$C_1$ parameter	<i>NSE on log of discharge</i>	$C_3$ parameter	<i>NSE on log of discharge</i>
-4	0.81	-0.3	0.68
-3.8	0.85	-0.25	0.79
<b>-3.74 (from data)</b>	0.86	-0.21	0.85
-3.7	0.86	<b>-0.2 (from data)</b>	0.86
-3.6	0.86	-0.19	0.86
-3.5	0.86	-0.17	0.86
-3.4	0.85	-0.16	0.85
-3.3	0.83	-0.15	0.83
-3.2	0.81	-0.1	0.45
-3	0.71	-0.09	0.26

3

4 Table 10. Comparison of the chosen parameter range and parameters obtained from low-  
 5 vegetation periods for the Ardèche at Meyras (#1) catchment.

Parameters	$C_1$	$C_2$	$C_3$
Parameter range	[-1] – [-6]	[0.1 – 1]	[-0.001]– [-0.5]
The range of “behavioral” values	[-3.5] – [-4.5]	[0.1 – 0.9]	[-0.001]– [-0.25]
Reference (from recession plots)	-3.74	0.65	-0.2

6

7 Table 11. Model performance for three examined catchments over the whole examined period  
 8 (2000–2008); Comparing the original operational data and rescaled precipitation and  
 9 evapotranspiration data.

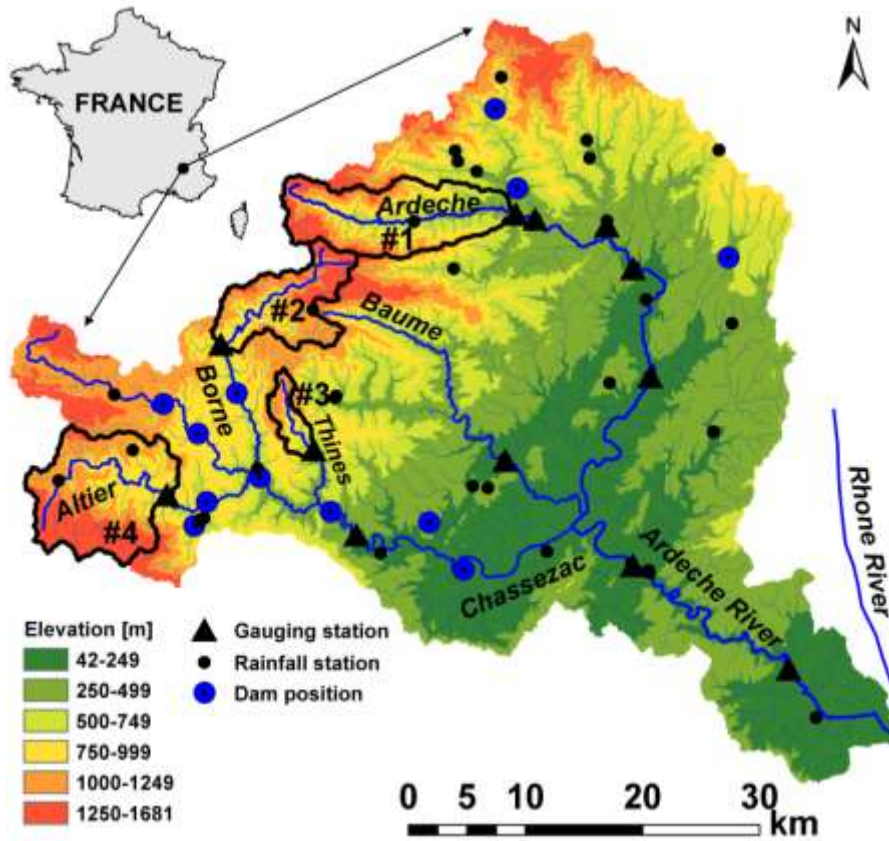
Catchment	Performance	Operational	Rescaled $P$	Rescaled $P$ and $AET$
<b>Borne at Nicolaud Bridge (#2)</b>	<i>NSE</i>	0.45	0.65	0.67
	<i>NSE log</i>	0.58	0.70	0.61
	<i>PBIAS</i>	42	14.2	0.75
<b>Thines at Gournier Bridge (#3)</b>	<i>NSE</i>	0.36	0.50	0.55
	<i>NSE log</i>	0.79	0.62	0.78
	<i>PBIAS</i>	-13.8	22	0.98
<b>Altier at Goulette (#4)</b>	<i>NSE</i>	0.54	0.79	0.74
	<i>NSE log</i>	-4.90	-2.99	0.18
	<i>PBIAS</i>	49	23.65	-0.29

10

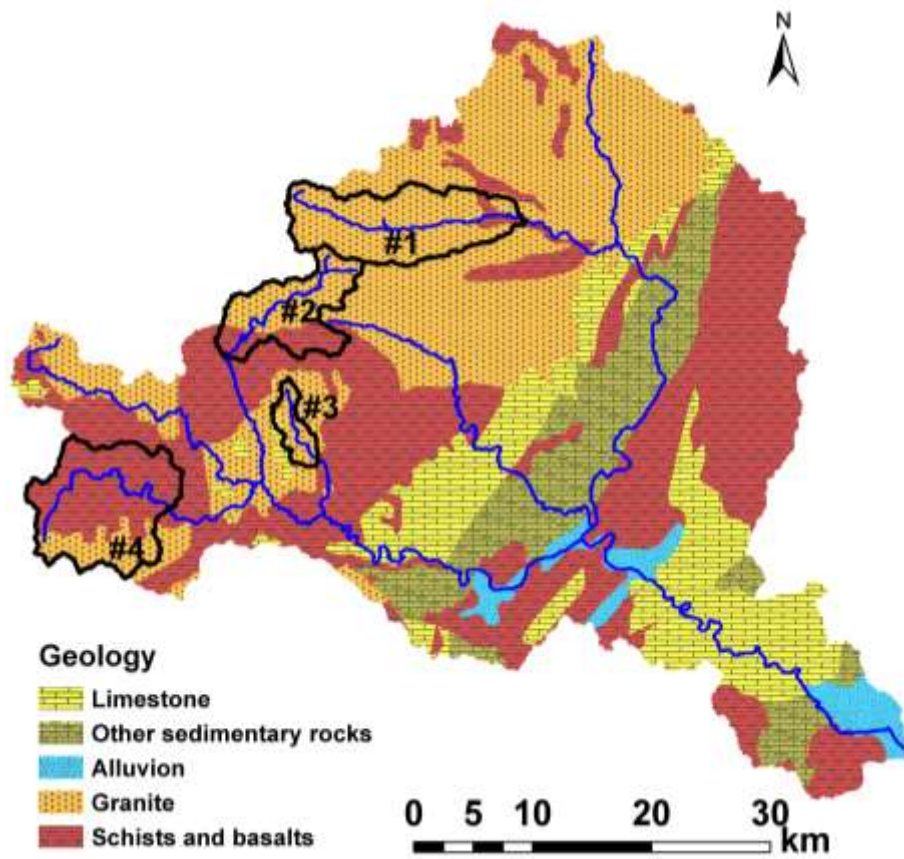
11

12

13



1  
 2 Figure 1. Map of the Ardèche catchment with gauging and rainfall stations, dam locations,  
 3 and catchments that were examined (in bold): #1. Ardèche at Meyras; #2. Borne at Nicolaud  
 4 Bridge; #3. Thines at Gournier Bridge; #4. Altier at Goulette



1

2 Figure 2. Geological map of the Ardèche catchment (extracted and processed from geological  
 3 map of France 1:1 000 000 issued by BRGM (6-th edition, 1996).

4

5

6

7

8

9

10

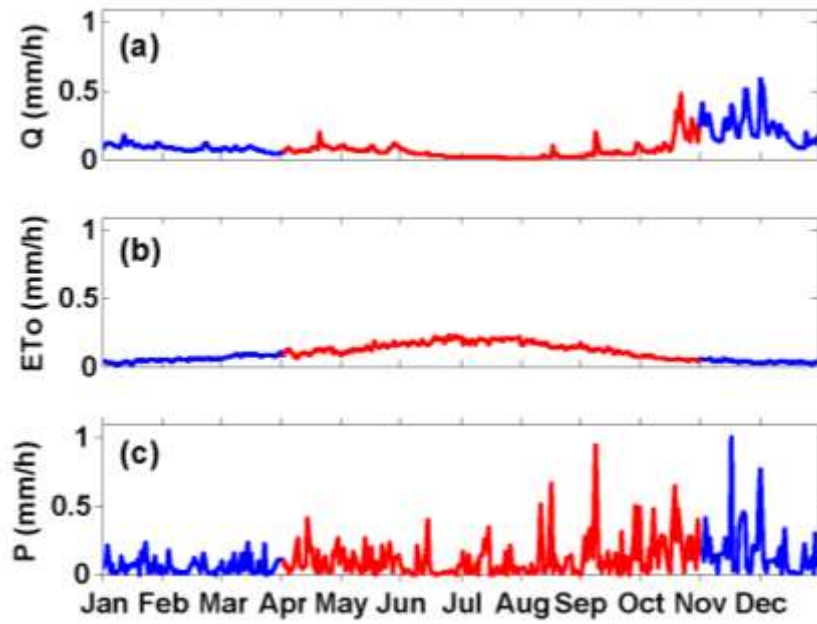
11

12

13

14

15



1

2 Figure 3. Average hourly discharge (a), reference  $ET_0$  (b) and rainfall (c) in (mm/h) at the  
 3 Ardèche outlet for all months between 2000 and 2008. (b) and (c) are calculated from the  
 4 SAFRAN reanalysis. In red: vegetation period; in blue: low-vegetation period

5

6

7

8

9

10

11

12

13

14

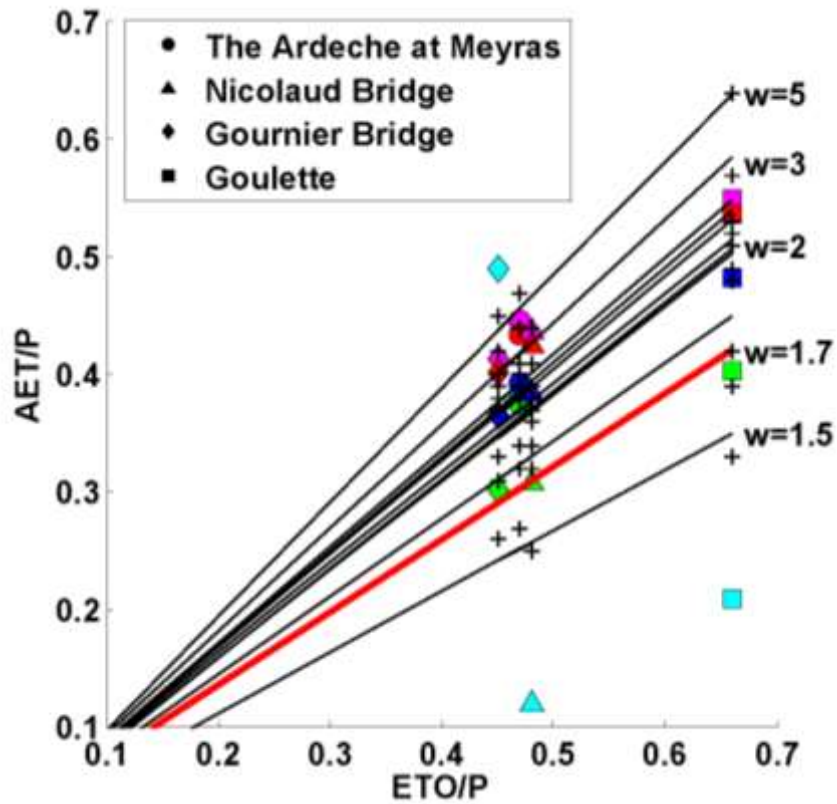
15

16

17

18





1

2 Figure 4. Mean annual evapotranspiration ratio  $AET/P$  as a function of the dryness index  
 3  $ET_0/P$  for different values of parameter  $w$ , using the Fu (1981) curve and different formulas  
 4 (Turc, Schreiber, Pike, Budyko; see Table 5). Colors correspond to different formulas  
 5 (cyan=original data; green=Turc, blue=Schreiber, pink=Pike, red=Budyko) and shapes  
 6 represent different examined catchments.

7

8

9

10

11

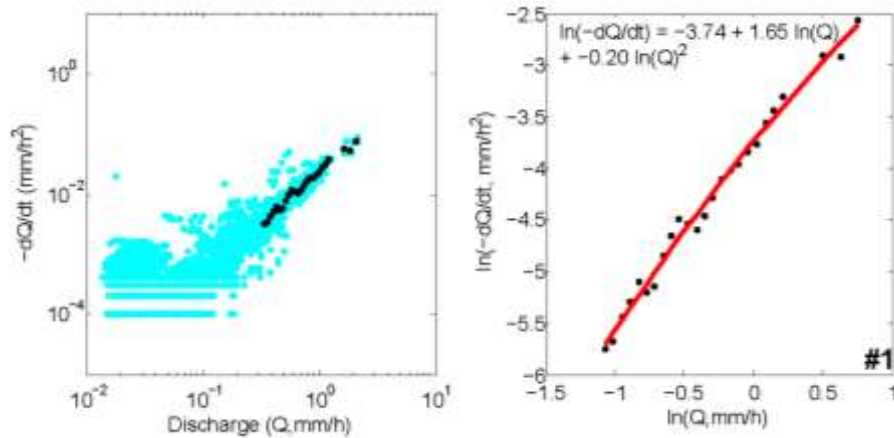
12

13

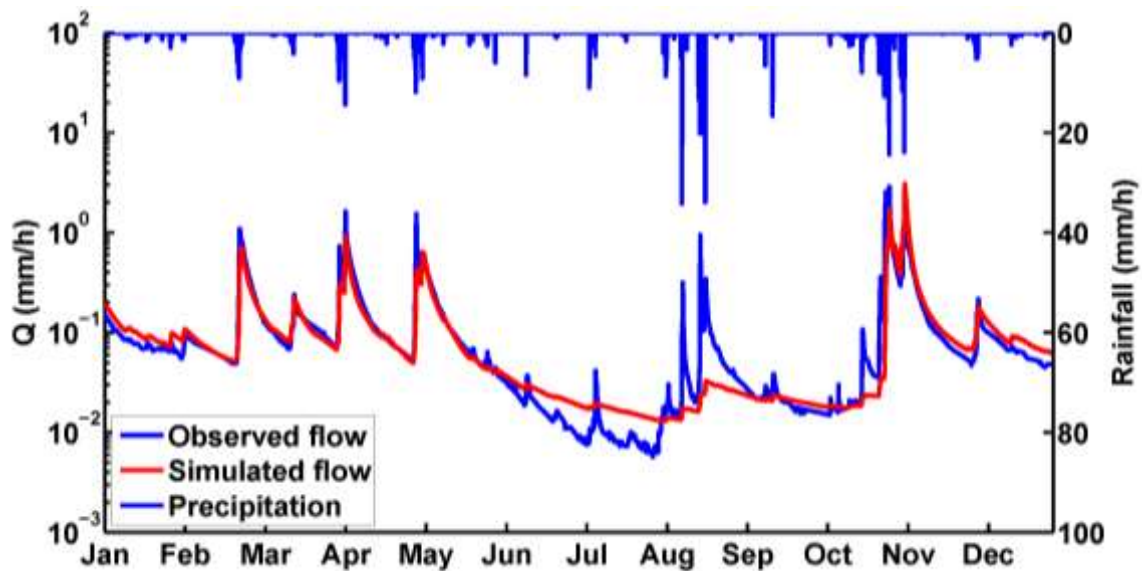
14

15

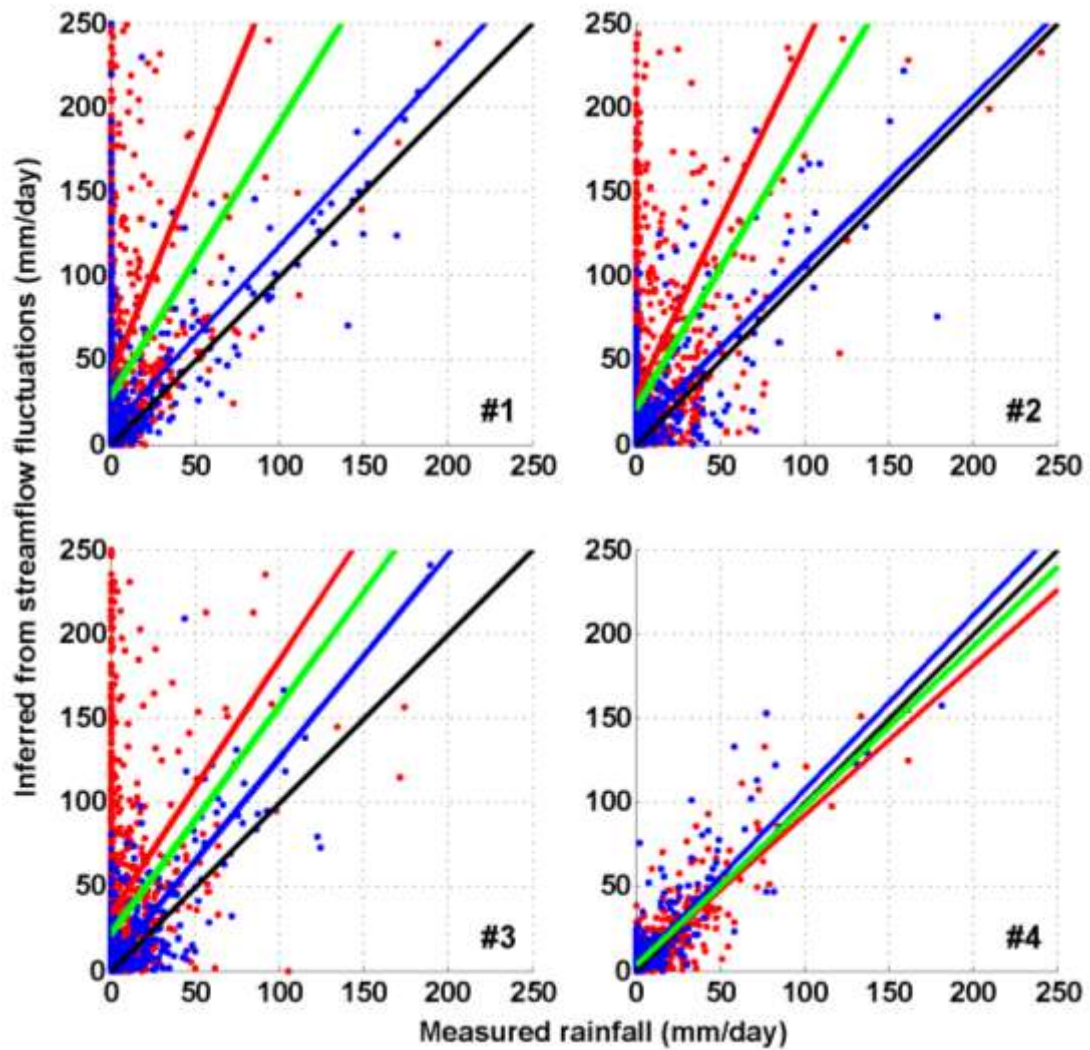
16



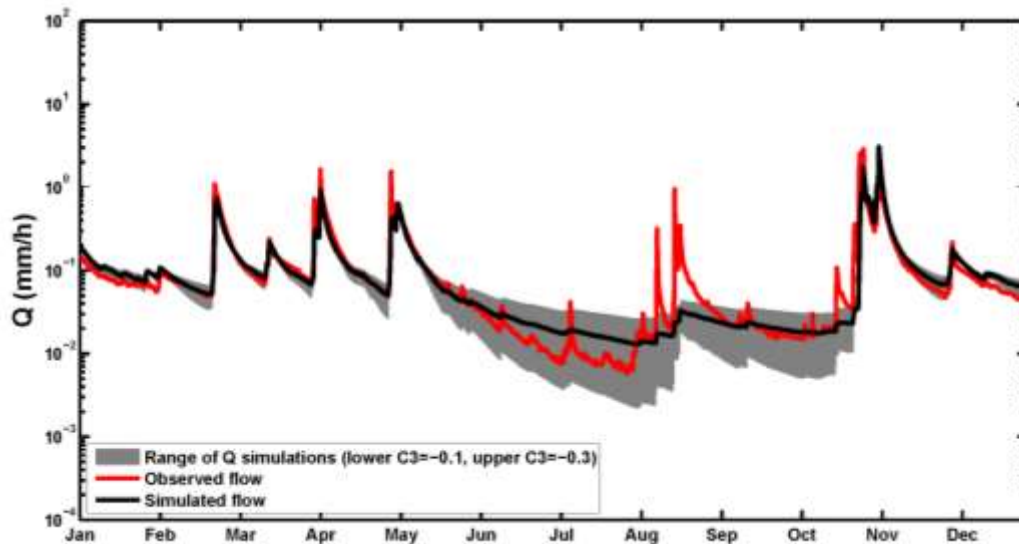
1  
 2 Figure 5. Recession plots for the Ardèche at Meyras (#1) catchment for all low-vegetation  
 3 periods between 2000 and 2008; (left) Flow recession rates ( $-dQ/dt$ ) as a function of flow ( $Q$ )  
 4 for individual rainless night hours (blue dots) and their binned averages (black dots). (right)  
 5 Quadratic curve fitting with binned means.



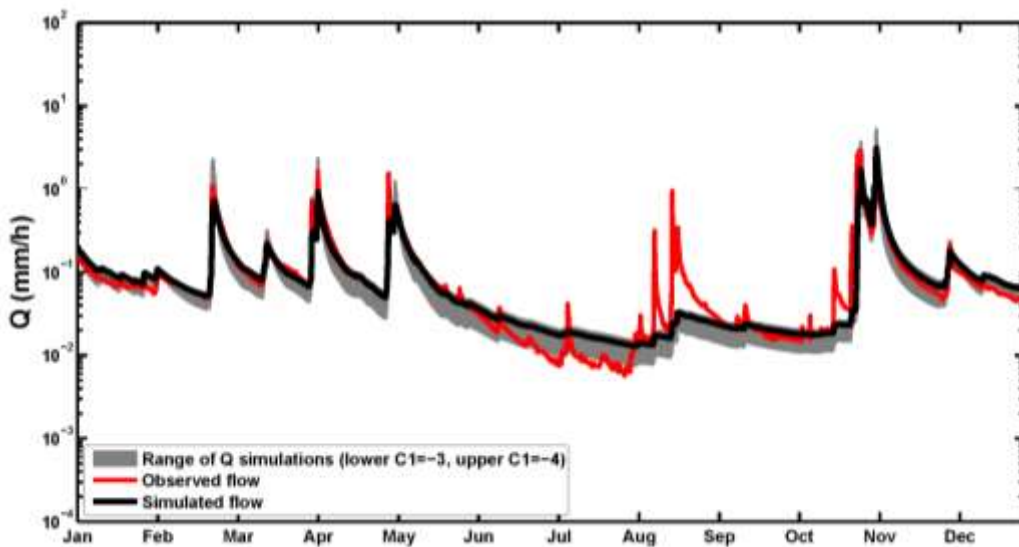
6  
 7 Figure 6. Series of simulated hourly hydrographs (red) for the Ardèche at Meyras (#1)  
 8 catchment for the year 2004, compared with observed discharge (blue).



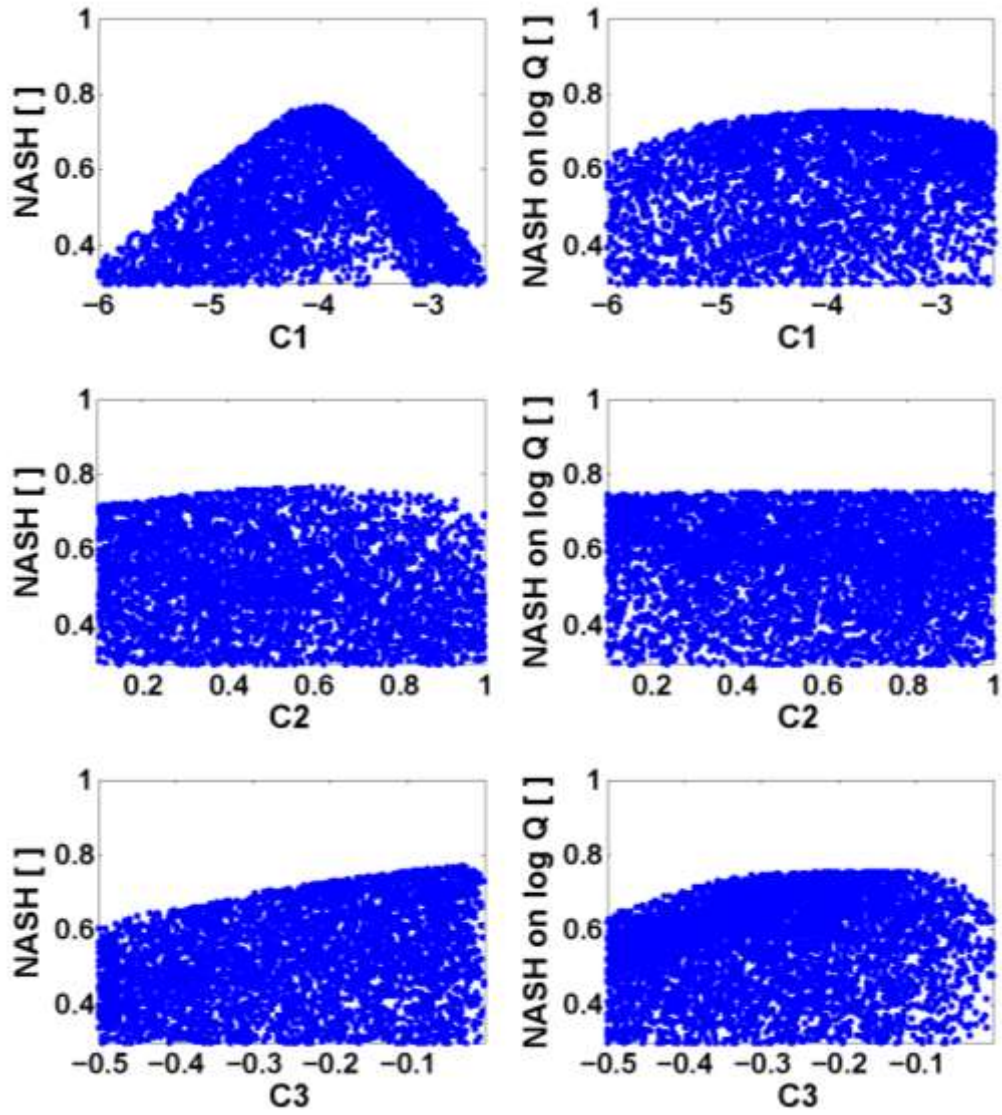
1  
 2 Figure 7. Inferred versus measured daily precipitation for the study catchments: #1. Ardèche  
 3 at Meyras; #2. Borne at Nicolaud Bridge; #3. Thines at Gournier Bridge; #4. Altier at  
 4 Goulette. Blue dots correspond to the inferred daily totals from low-vegetation periods; red  
 5 points correspond to the inferred daily totals from vegetation periods; blue line is correlation  
 6 for low-vegetation period, red line for vegetation period and green line for total examined  
 7 period.



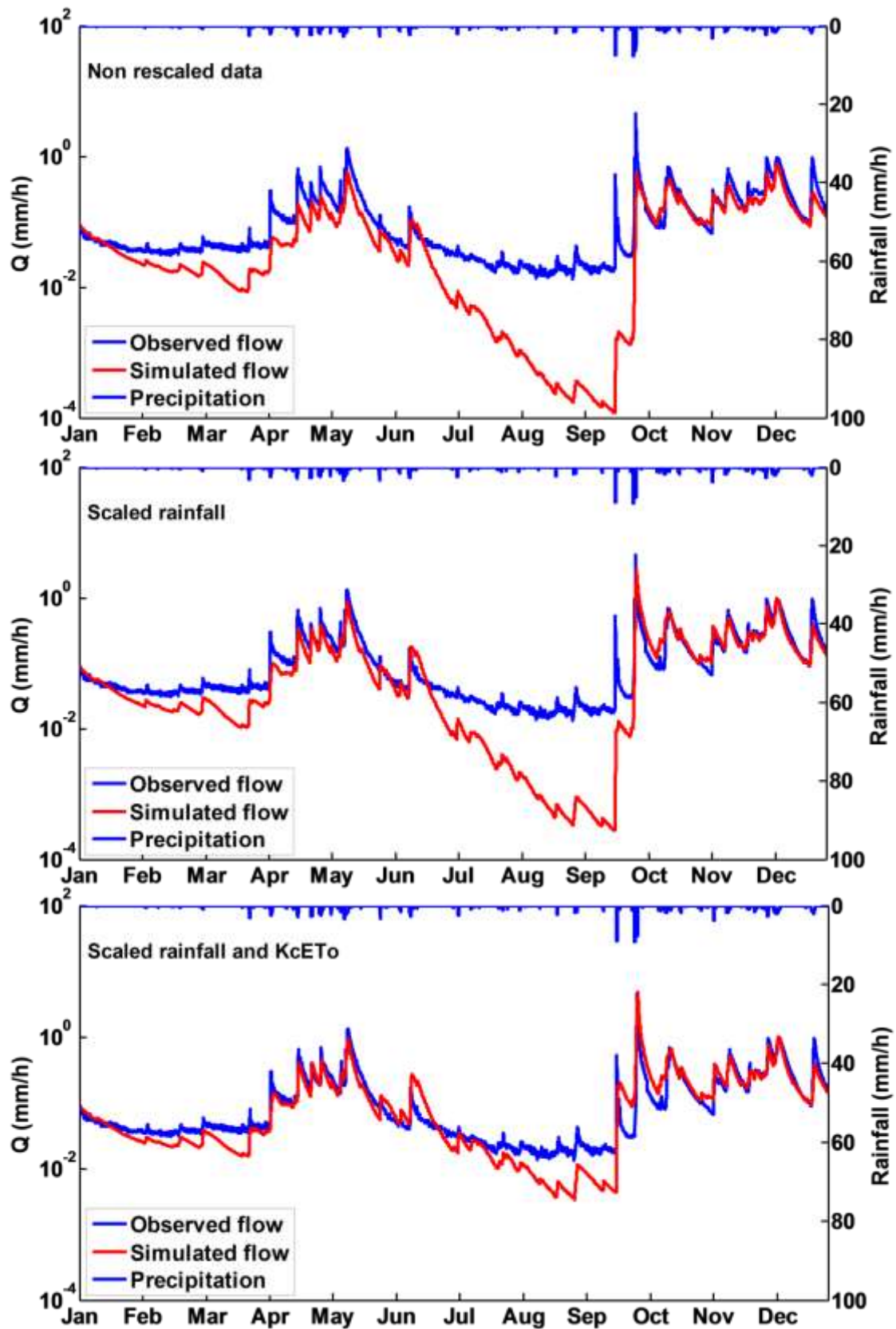
1  
 2 Figure 8. Observed versus simulated hydrograph ( $C_3=-0.2$ ) for the Ardèche at Meyras (#1)  
 3 catchment (year 2004), with  $C_3$  parameter variations ( $C_1$  and  $C_2$  values are kept constant at (-  
 4 3.74) and 0.65, respectively). The grey area shows the range of discharge simulations.



5  
 6 Figure 9. Observed versus simulated hydrograph ( $C_1=-3.74$ ) for the Ardèche at Meyras (#1)  
 7 catchment (year 2004) with  $C_1$  parameter variations ( $C_2$  and  $C_3$  values are kept constant at  
 8 0.65 and -0.2, respectively). The grey area shows the range of discharge simulations.



1  
 2 Figure 10. Dotty plots for the Ardèche at Meyras (#1) catchment (left: plots with *NSE*  
 3 efficiencies; right: plots with *NSE* efficiencies calculated on  $\log Q$ ).



1  
 2 Figure 11. Series of simulated hourly hydrographs (red) for Altier at Goulette (#4) catchment  
 3 for the year 2000 and its comparison with observed discharge (blue), using original non-  
 4 scaled data (top), with rescaled  $P$  only (middle), and rescaled  $P$  and  $K_cET_0$  (bottom).